

Chapter 1 Introduction

1.1 Brief introduction to EDM

For the past decades Electrical discharge machining (EDM) technology has been gradually evolved and it becomes one of the most important manufacturing processes. Electrical discharge machining (EDM) is an unconventional machining process that developed back in 1770s by English scientist but only after 1940s it was universally accepted when Russians studied and controlled the spark and erosion effects on the materials. Unlike Traditional methods that required hard tools for material removal, EDM works on thermoelectric process where hot plasma channel causes the melting and vaporization of the workpiece. EDM is a contactless manufacturing process that is used to machine conductive materials accurately, precisely and cost effectively [1]. Due to some limitations like lack of flexibility to machine complex & intricate parts, pre-shaped tool fabrication and high tool cost traditional EDM or die-sinking EDM inspite of being most popular non-traditional manufacturing process limits its capabilities. There are mainly two types of EDM viz Die sinking EDM and WIRE EDM, as shown in Fig. 1.1. In Die Sinking EDM, tool electrode had reverse shape of the feature to be machined, while Wire EDM, tool electrode is a thin wire of zinc coated brass or other suitable material.

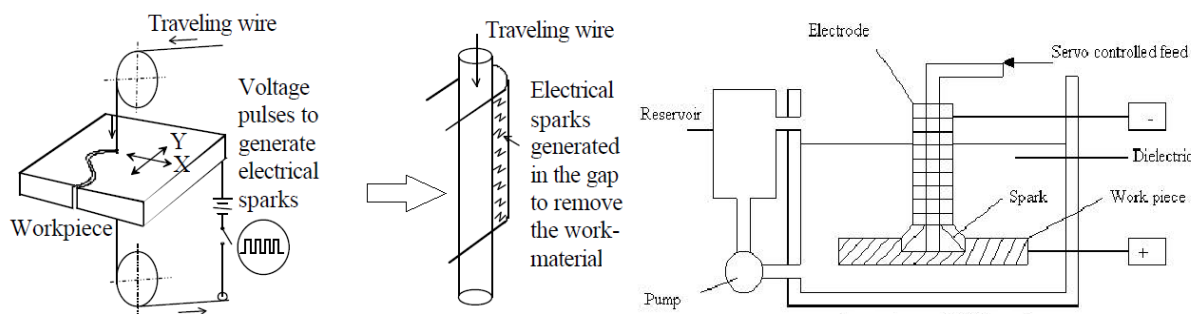


Fig.1.1 Types of EDM (WEDM and die sink)

Discharging of energy occurs through four ways depending upon the type of gap conditions. There are four types of gap conditions namely short, open, spark and arcing. Short occurs when the distance between both electrodes is negligible or debris filled the gap or when they have direct contact; when two electrodes have enough gap between them the open voltage conditions occurs as no current recorded; sparks are preferred and is a desirable condition for

a operation to occur and arching is the condition to be avoided as it deteriorates the surface quality and dimensioning. Fig. 1.2 shows different V-I characteristics for the gap conditions.

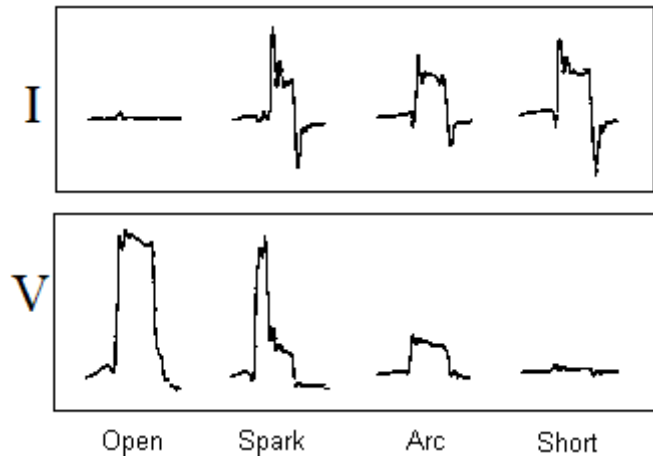


Fig. 1.2 V-I Characteristics [23]

1.2 Principle of Thermoelectric erosion

A series of non stationary and transient sparks occurs between the electrodes i.e. tool and workpiece separated by a small gap usually controlled by a servo unit called spark gap in order to avoid the short circuit. At a particular maximum point where spark gap is minimum breakdown of dielectric occurs, voltage falls and current increased instantaneously and as a result of avalanche of electrons plasma channel forms between the electrodes and due to very high temperature of 10,000 to 12, 0000 °C, melting and vaporization of the workpiece takes place. As material removal occurs comparatively more at anode than cathode so usually workpiece is made as anode and tool as cathode. Both Tool and workpiece always remain surrounded by dielectric fluid. After machining, flushing of the dielectric is made in order to remove the debris (molten material) and remaining unexpelled molten material forms a recast layer on solidification. In this way material is removed in a single electric spark and the system is ready for the next series of 1000 sparks per second. In this way uniform erosion of material takes place at the end of machining in a precise and controlled manner.

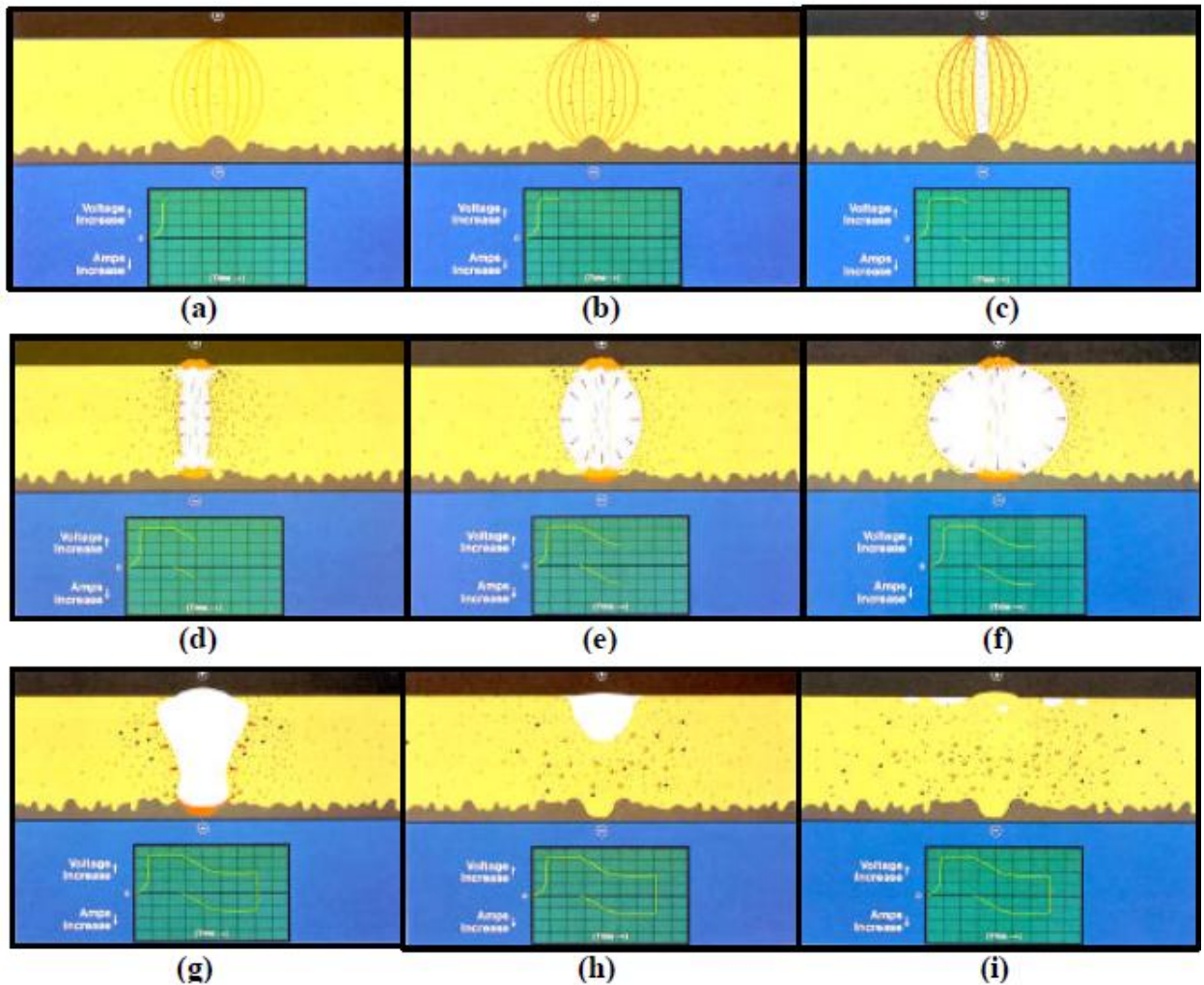


Fig.1.3 Thermoelectric principle [24]

1.3 Brief Introduction to WEDM

Wire electrical Discharge machining (WEDM) is unique version of EDM with similar traditional EDM working principle of thermoelectric erosion except the tool electrode which is replaced by a thin continuously moving wire as shown in Fig.1.4. In 1969 Swiss from Agie produced first ever WEDM machine and in 1974 first time D.H. Dulebohn operate the WEDM for machining and controlling the shape of the workpiece with the help of optical line follower. By the end of 1970s with the advancement in technology and evolution of computer numerical control (CNC) system, WEDM mark the major revolution in the field of machining due to its broad process capabilities. WEDM gains the popularity due to its unveiled potential that can be applied in various industries like aerospace, biomedical, production, marine etc that involves the machining of conductive materials. WEDM proves to be the best alternative to machine the conductive, exotic, hard to machine and temp-resist

metals, composites, superalloys etc in a precise and highly dimensional form to generate from simplest to most complex geometries [2]. Fig. 1.5 shows the Block diagram of WEDM setup.

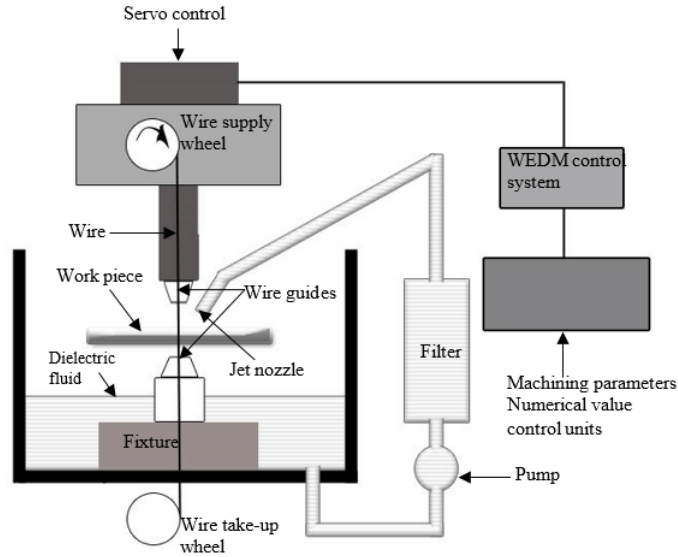


Fig. 1.4 Thermoelectric Principle in WEDM [25]

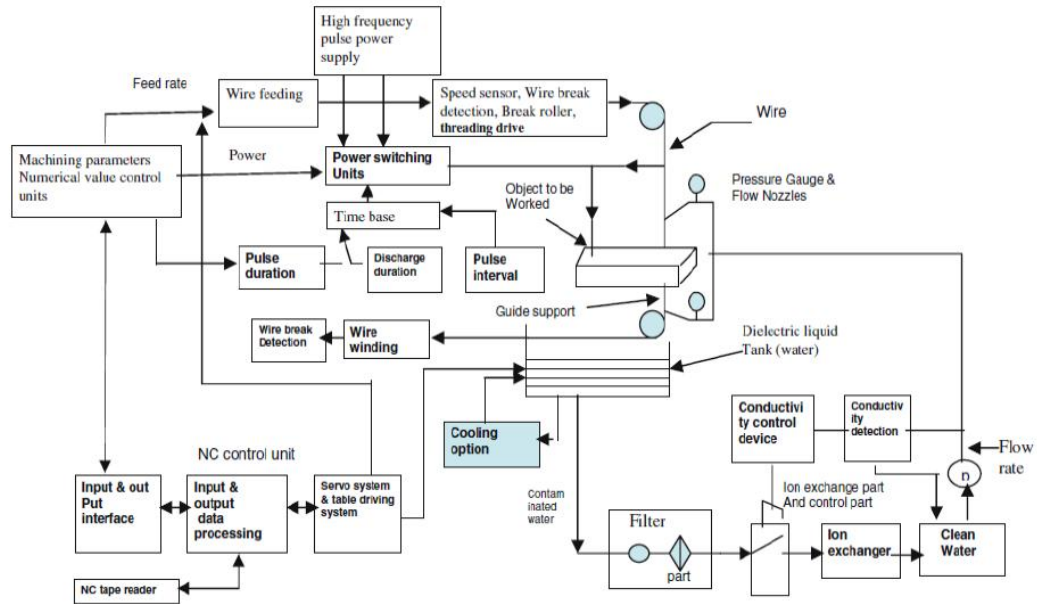


Figure 1.5 Block diagram of WEDM (26: Mahapatra et al., 2007)

1.4 Classification of WEDM

Flushing Type WEDM and Submerged type WEDM are two basic types of WEDM setups.

- Flushing Type WEDM:

Flushing type WEDM uses the splash of dielectric continuously during the machining in a restricted zone area where spark occurs. Nozzles are located at upper and lower guide that throw out the jet of dielectric with high amount of pressure in order to make a complete channel. It is used in the mostly setups that involve R & D work or small level work. usually, these WEDM is not suitable for large size workpiece , hence in mostly industrial uses these machines are not used. One of the great advantage of these machines is that it allows an operator to see the process of machining by naked eyes while performing, it helps sometimes to reduce errors.

- Submerged Type WEDM:

Submerged type WEDM offer great advantages over the flushing type as it can accommodate large size of workpiece and hence most popular for industries and large scale work. In this type , Work material fully submerged into the dielectric fluid kept in the dielectric tank. It increases the efficiency of the process and reduces the hazards caused on workpiece during machining. Submerged type can be used substitute the Flushing type, while flushing type can't replace the submerged type. It is useful for applications that have poor flushability. Some typical applications include taper angles, laminations, tubes, irregular shaded parts and cutting very close to edge of the workpiece.

1.5 Cylindrical turning in WEDM

Cylindrical Wire electrical discharge turning (CWEDT) is a unique adaption of WEDM in which an additional rotary axis is added to the conventional WEDM setup. CWEDT in addition to the machining of intricate shapes and complex profiles, it also enables the turning of workpiece, machining of intricate profiles and generation of cylindrical, helical, spherical forms and geometries in a smooth way [3]. In CWEDT, the workpiece is made to rotate axially against the transverse motion of the wire, which removes the material through melting and vaporization. Work piece rotational speed and frequency adds an important parameter that governs the roundness and shape of geometries produced by CWEDT along with other parameters like wire tension, wire speed, wire feed, peak current, pulse duration (Ton), pulse interval (Toff), gap voltage, sensitivity and dielectric flow rate. It is best suitable to generate 2D and 3D complex and intricate geometries with small corner radius of high surface

integrity on exotic metals and alloys that are wear-resistant, hard to machine like superalloys, composites, polycrystalline diamond, CBN etc. Fig. 1.5 shows the CWEDT

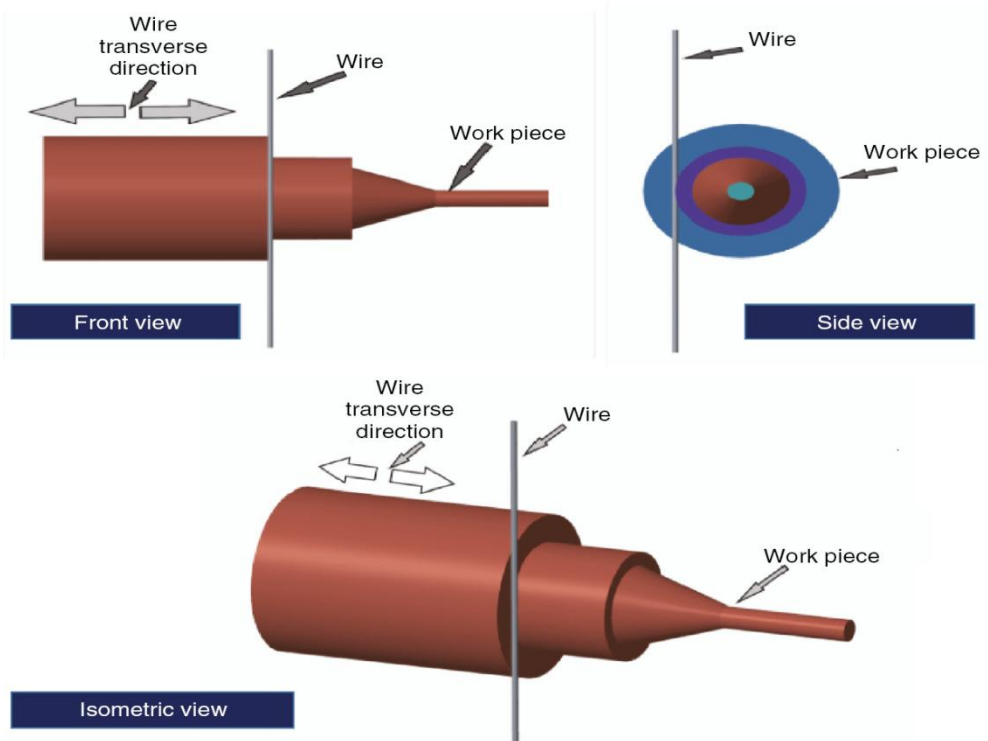


Fig. 1.6 Cylindrical Turning concept in WEDM [17]

1.6 Working principle and components of CWEDT

Basically CWEDT principle is only a thermoelectric erosion process, on which WEDM works, Spark is generated between the travelling wire and rotating workpiece and erosion of the workpiece occurs as per thermoelectric principle.

1.6.1 Components of WEDM:

1. Power supply unit

This unit usually consists of electric pulse generator switch, DC motor to drive and position X, Y, U and V Axes. Recent development of AC system that replaces the DC eliminated the blue-discoloration that is caused on the surface of titanium and nickel alloys upon machining. Improved power options also minimized the benching, hand polishing or lapping of the parts due to increase in the surface quality due to the optimum and quantified flow of discharge energy during machining which finally able to generate very fine finish with good quality surfaces. Power changes, servo motor timings, spark

sensitivity are improved due to the high speed circuitry due to the addition adaptive control systems

2. Computerized Numerical Control (CNC)

It acts just like a brain for a human body. Numerical control is made these days according to the operators demand and feasibility. Control unit displays the list, functions, operations list, workout data and machining axes movement. Characters and commands are entered through the keyboard or touch panel. Serial communication of programs is also been compatible with the CNC system with the help of the software's like Elcam etc. Nowadays , modified machines replaces the floppy disc storage with the direct Pen drive or USB port through which operator can directly input the program to the setup .

3. Feed and Drive mechanism

DC servo motors are used to drive the main table on which the work piece is clamped. Constant feed rate of wire is maintained between upper and lower guides. when the WEDM was first used copper wire was used but soon after some years limitations of the Cu wire is realized due to increasing need to high speed and large no of forces. low tensile strength and poor flushablity are the major drawbacks of the Cu wire. Due to large amount of heat dissipation in the wire, wire needs to be more thermally strong with high tensile strength. Nowadays there are array of wires available of different materials but usually Brass with Zinc coated is the most popular and used one, other includes molybdenum, graphitized, and thick and thin layered composite wires.

Automatic wire threading (AWT) is a recent advancement to the wire system of the machine; This will add an advantage to allow multiple openings to cut in die blocks, productions and prototype workpiece automatically. This also reduces the operator intervention during the wire breakage and overnight operations. AWT increased the productivity of the process and machine.

4. Positioning and Control system

Positioning and control system mainly consist of Main worktable of X and Y-axis on which the workpiece is clamped, Auxiliary table of U and V-axis for the independent inclination of the wire from the main table and the wire drive mechanism. Taper can be provided on complex profiles using the wire inclination axes with range of $\pm 45^\circ$. Taper angle can be changed for the form tools and dies that have different front and side relief angles. Helical, conical and cyloidal shapes can machined with the proper adjustment and alignment of the tables.

5. Dielectric system

Dielectric system consists of the water reservoir, filtration system, de-ionization system and the chiller unit usually. Generally it is similar to the Vertical EDM system except for the dielectric fluid i.e. HC or mineral oil used in traditional EDM is replaced by the De-ionized water in order to control its conductivity. Continuous flow of the dielectric on both the sides of the workpiece from two high pressure jets is maintained by the proper flushing system that controls dielectric flow rate for the both jets nozzles individually.

6. Rotary System

Transverse to the wire motion, spindle rotary axis is added on the main worktable. Spindle should be accurate and flexible in order to minimize the spindle error.



Fig. 1.7 Rotary spindle system

1.7 CWEDT advantages and applications

Applications includes shafts of turbocharger, diesel injector pump, splines, miniature parts, Instrumentation spindles, probes, biomedical tools, pumps actuators, turbines needles etc. CWEDT possess tremendous capabilities for achieving high dimensional finish in complex cylindrical geometries that are used widely in modern and heavy industries. Although several researches have been done to optimizes the CWEDT process for better output responses. Since last decade its unique capabilities with technology advancement have proved to be one of the greatest and successful machining processes that not only encompass the limitations of conventional turning and other finished operations like grinding, broaching etc.

Due to the use of different kind profile parts of various shaped geometries in modern applications like aerospace, medical and automobiles. In this research project CWEDT process is thoroughly studied and its parameters are investigated for the better surface integrity of the different geometrical profiles machined by CWEDT.

Chapter 2 Literature, Motivation and Objective

Need for precise geometries and complex 3-D shaped miniatures or assemblies have made CWEDT an important machining process. CWEDT is basically a WEDM process with some additions, with common advantages and disadvantages. Although the importance of WEDM was realized in 1970s onwards but CWEDT capability and importance was realized usually 2005 onwards due to increasing demand of complex cylindrical geometries and intricate contours in the modern industries that works on advanced or exotic engineering materials.

Following chapter deals with the highlights of development associated with past research work and analysis. Literature Review usually contains problem-solving strategies or methods, new findings and improvisations (or optimization) done by the researchers in the last decade. It also underlying the critical problems and appropriate research gap associated with the existing research.

2.1 Research papers on CWEDT are arranged below on the basis of development and approaches adopted. Some papers on EDM and WEDM are also accompanied below with CWEDT that are important in context of this study.

- Dhake and Samuel [3] customize WEDM setup by adding a rotary spindle system to make workpiece to rotate for cylindrical turning of the round shaped workpiece. CWEDT is done to generate axi-symmetric form and complex profiles like helical shaped. Geometric deviations and surface investigation is done for the axi-symmetric and helical shaped profile. Observation shows the min and max dimensional error of 0.10 and 3.10 % respectively for axi-symmetric forms. Helical shaped profile shows the maximum variation of mean pitch measured is 0.031mm and maximum standard deviation is 0.028 mm. Work also reported some tapering of the profiles and the reason stated was the set-up errors and eccentricity of the spindle axis.
- Magabe et al. [4] uses WEDM process to machine the Ni55.8Ti shape memory alloy. Experimental investigation is done to study the influence of gap voltage (GV), pulse-on time (Ton), pulse off time (Toff) and wire feed (WF) on the MRR and surface roughness i.e. mean roughness depth (Rz). Taguchi's L 16 and Non-dominated sorting algorithm-II (NSGA-II) is used for DOE and process optimization respectively. Observations revealed GV, Ton and WF as in direct relation with MRR with Ton being the most significant parameter, while Toff shows the inverse relation with

MRR. Surface roughness (Rz) increases with GV, Ton, WF and decreases with Toff. NSGA based on crowding distance optimization gives the sets of optimal parameters that are needed to check against the best result. Confirmation results at predicted optimal setting shows improve in the surface quality (Rz-6.20 μm) and process productivity (MRR-0.021g/min) in a single set.

- Kumar et al. [5] improved MRR of Inconel 825 in case of EDM process by adding Al₂O₃ nano-powder in dielectric fluid while machining with rectangular cross section copper tool electrode. From the waveform of discharging process it is clear that powder particles addition in dielectric decrease the arcing during the process which causes improve in MRR and SR by 44% and 51% respectively in contrast to normal EDM process.
- Muthuramalingam et al. [6] studied the recast layer of AISI 202 steel which is machined in EDM process by tungsten carbide and brass tool electrode, as the tungsten carbide is harder than brass and EDM involves erosion of both electrode so a hardened recast layer is deposited on the top surface of workpiece when using tungsten carbide on the opposite hand brass tool decrease the hardness of workpiece.
- Qu et al. [7] [8] were the first to perform experiments for CWEDT in two phases as part 1 and part 2. They demonstrated the machining of the free-form cylindrical geometries by applying CWEDT. Materials selected were brass and carbide. Experiments were conducted in two configurations for each cylindrical WEDM and 2D WEDM. For cylindrical $\alpha=0$ and $\alpha=\text{constant}$ are taken as 2 configurations respectively. For 2D WEDM, straight cutting is done only in both the configurations but cross sections were varied. They also investigated the spindle error at different spindle speeds (N) and state it as an important parameter affecting cutting rate, roundness and surface integrity.

In part 1, authors derived the mathematical model for MRR and calculate MRR for both configurations. Results showed that the MRR of CWEDT is higher than that of simple 2D WEDM due to better flushing conditions.

In part 2 Mathematical models for surface finish were introduced and expression for mean surface roughness (Ra) was derived. Two sets of experiments were conducted. In exp 1, at high MRR, Part rotational speed (N) & wire feed rate (V_f) were varied and 24 runs are performed for investigating the surface roughness and roundness. Observations showed, surface roughness Ra & Rz decreases at higher N and lower V_f .

Also Part rotational Speed N has very less significance on Roundness and high Roundness at lower V_f due to low vibration error. In Exp 2, Pulse ON time and V_f are made to vary for max possible surface finish and roundness. Better surface finish and roundness are recorded at lower Pulse ON time and lower V_f due to smaller sparks.

SEM Micrographs also analyzed for macro-ridges, craters, HAZ (s) and their Sizes were recorded. Results also showed the decrease in MRR for experiment set 2 than set

1. Authors successfully modeled the process for better Surface integrity and Roundness of CWEDT machine parts.

- Haddad et al. [9] performed Wire electric discharge turning (WEDT) on AISI D3 tool steel. Parameters taken were Pulse off Time (Toff), Voltage (V), Power (P) and Spindle speed (N). Classical Design of experiments (DOE) and Taguchi Method were integrated and the experiments were performed using L9 orthogonal array with three replicates, making total 27 runs of experiments. Straight turning is performed and output responses like Material removal Rate (MRR), surface Roughness (Ra) and Roundness were calculated. ANOVA technique is employed for determining the behavior of the parameters and parametric optimization is preformed using SN ratio values. Output Responses Equations were calculated using Regression analysis for performance modeling. Results shows direct proportionality of P and V and reverse proportionality of Toff and N for MRR. Voltage (V) being the most significant and Spindle speed (N) comes to most insignificant parameter. For Surface roughness, Power (P) shows the most significant effect followed by V, Toff and N. Like MRR, Toff and N shows reverse proportionality for Ra i.e when value of Toff and N increases value of Ra decreases. Similarly for Roughness Toff and N shows reverse effect and are only significant parameters. SNR values are used to obtain the optimum parameters and in turn confirmation experiments are performed in order to validate the model. MRR increases by 1.11 times, Ra decreases by 1.3 times and Roundness decreases by 1.226 times.
- Haddad et al. [10] investigated CWEDT on AISI tool steel for Roughness(Ra) and Roundness by optimizing the process parameters like pulse off time (Toff), Voltage(V), Power(P) and Spindle speed (N). Full-Factorial technique is used to design the experiments. Power and Voltage shows increasing nature with increase in Ra values while N and Toff shows reverse nature. Power being the most significant factor. In case of roundness, N shows the most significant effect followed by V and

also Toff being the most insignificant factor. RSM surface plots shows at higher N, if voltage is increased then Roundness increases significantly. SEM analysis of the cross sections shows the deposition of Chromium carbide on the microstructure, macro ridges, craters and recast layer thickness at various discharge energy values. EDAX shows the Cu and Zn elements in the Recast layer. Micro-Hardness is measured for the machined surface and found to decrease significantly in HAZ as compared to the bulk. Further researcher concluded that the Discharge Energy is the controlling parameter that affects the HAZ and recast layer thickness.

- Haddad et al. [11] performed MRR modeling for the CWEDT AISI Steel. Parametric effects were analyzed using ANOVA, Surface plots and regression equations are generated using RSM technique. Finally Microhardness test and SEM analysis of the machined samples is done. Power and Voltage being the most influential factors have the direct proportional relation with MRR. For the Maximum MRR, values of both the parameters Power (P) and Voltage should be high, also Pulse Off Time (Toff) and speed (N) as low as possible. craters, macro ridges, cut-offs , HAZ and recast layer is investigated and found to be highly depend on Power and voltage i.e. discharge energy. Microhardness is also calculated and found to decrease in HAZ due to high Discharge energy.
- Mohammadi et al [12] develops novel hybrid technique combining ultrasonic vibration with the cylindrical WED Turning. Auxiliary device causing ultrasonic (US) vibrations is installed between two guides, makes wire to vibrate at resonance mode. Material removal rate (MRR) and surface roughness (Ra) investigation is done on HSS work piece of hardness 64 ± 2 HRC. Full factorial design technique is used to design the experiments and ANOVA is used to study the significance. Finally 3D surface plots are used to show the behavior of the parameters and their interactions on the MRR. Observations shows Power and Ultrasonic vibrations are the most significant factors in improving the MRR with their increasing levels followed by the Spindle rotational speed. Also, Pulse-off Time (Toff) shows reverse relation with MRR. Reasons stated by the author for increased MRR using US-Vibrations are improved Flushing conditions, causing easier discharge breakdown with the creation of cavitation. Surface roughness (Ra) found to increases with the power. In order to obtain good surface finish with higher MRR, parameters were optimized as power 3A,

Toff 12 μ s, Spindle speed 45rpm and ON condition of US vibrations. Finally obtained Responses were MRR 0.72976 mm³/min and Ra.1.810 μ m.

- Mohammadi et al [13] integrated ultrasonic system is in conventional WEDM setup which is assisted with a rotary spindle for the workpiece rotation. Surface integrity and Crater analysis is done on single discharge basis. Mixed Level Factorial $2^3 \times 3^2$ DOE technique is used for selected parameters viz. Power (P), Ultrasonic Vibration (UV), Pulse-off (Toff), workpiece rotational speed (N) and ANOVA is used to show their significance. Observation showed better surface with high MRR at low power and higher levels of Toff, N with assistance of ultrasonic vibrations (UV). Reduction in recast layer, HAZ and micro cracks at same discharge level with UV are observed in SEM. Decrease in the length of crater and increase in width due to induced UV causes more material removal per discharge.
- Mohammadi et al [14] investigated ultrasonic assisted CWEDT. Modelling and optimization of the parameters like Power (P), Pulse-off time (Toff), ultrasonic vibration(UV), spindle speed (N) for the MRR, surface Roughness (Ra) and Roundness (R) is performed. CCD of RSM technique is used for DOE and ANOVA is employed to study the effects. Finally multi-objective optimization is done. Optimal settings corresponding to max MRR, Min Ra and Min R are obtained as Power = 2A, Toff=8.106 μ s, V=130V, N=45RPM, UV amplitude=11.857 μ m. Experimentally verifying the predicted optimal values shows the error 4.24, 6.1, 4.8 % for MRR, Ra and R respectively. Significance of UV amplitude is validated for MRR but Ra and R are less affected by UV amplitude.
- Janardhan and Samuel [15] uses pulse data acquired at the spark gap using a data acquisition system to analysis MRR, Surface roughness (Ra) and roundness error of the CWEDT samples. .MATLAB is utilized in making the Pulse classification algorithm for the off-line analysis of WEDT. Observations showed the workpiece rotation causes the arc regions in WEDT. Type of discharge, duration and no of discharge has significant effect on the MRR. Nearly 50 % increase in MRR is found on decreasing the Spark gap and pulse-off time. Surface Roughness (Ra) found to increase with increase no of the arc regions and with the decrease in the ignition time delay. With decrease in pulse-off time, spark gap and servo feed, reduction in the Surface roughness (Ra) is found as 56 % of the total reduction, 43% and 22% respectively. Furthermore Roundness error shows highly dependency on Pulse-off

time by showing 74% reduction with the decrease of pulse-off time. Increase in the workpiece rotation speed also reduced the error by 17%. Also roundness error decreased with reduction in the no of arc regions /time.

- Giridharan and Samuel [16] proposed a new model to calculate the Erosion rate of each spark for the given Discharge Energy (DE). AISI 4340 is chosen the work material and Discharge Energy is chosen the only input parameter. In the proposed model, crater diameter is calculated using a derived analytic expression. Erosion rate is finally found by measuring the Crater depth using the 2D-surface profilometer. 3D surface Topography is used to validate the predicted erosion rate for the experimental data. For lower DE (<2J) predicted erosion rate comes in good proximity with the experimental results but for higher D.E, model over-predicts. Furthermore it is stated to use the proposed model in determining the erosion rate for hard materials prior to performing experiments. Also, for any axi - symmetric component proposed model can be used at a given DE for controlled crater erosion.
- Sun et al. [17] fabricate the microelectrode of 90 μm diameter and 1000 μm length using LS-WEDM. Multiple cutting strategy is adopted and surface analysis is performed. Surface Topographic Observations showed large no of ridges and black accretion after the rough cut (RC), Spherical congregated droplets after the trim cut (TC) and a refined layer of grains at the nano level after the finish trim cut (FTC). Furthermore, comparative study is done for LS-WEDT and LS-WEDM machined surface for each cutting strategy. Surface roughness (Ra) obtained of LS-WEDT surface is larger than LS-WEDM surface for the RC due to ridges and deposition; but Ra of LS-WEDT is smaller than LS-WEDM after FTC due to better flushing conditions and point contact discharge phenomenon. Finally, fabricated Microelectrode is of better quality surface and precise form with $\text{Ra}=0.59 \mu\text{m}$.
- Sun et al. [18] manufacture and fabricate the ultra micro-electrodes using LS-WEDT. Bending and Breaking phenomenon of the micro-electrodes is analyzed and found to be greatly affected by discharge energy, Flushing pressure and open circuit voltage. Proper selection and adjustment of the parameters is of much importance to avoid this. Lower F.P, lower OCV. Lower peak current in altogether decrease the discharge energy that finally prevent the distortion and failure of the micro-electrodes finally microelectrode of 58 μm diameter is fabricated with lowered optimized parameters with good surface finish and high precision and without inclination and waviness.

beside ultra microelectrode, Micro-cutting tools of D-shaped of 65 μm diameter and 3-spiral shaped tool were fabricated first time using LS-WEDT . It also proved the competence of LS-WEDT with WEDG for the complicate profiles.

- Gohil and Puri [19] performed Electrical discharge turning of hard to cut materials with good precision and accuracy is achieved using conventional die-sinking EDM assisted by a precise spindle arrangement to rotate the workpiece. Shaped conductive copper strip is made to feed the workpiece in order to generate axi-symmetric geometries. Experimental investigation of Ti-6Al-4V under the influence of flushing pressure (FP), gap voltage (GV), peak current (I), pulse-on time (Ton) and spindle speed (N) is performed under the reverse polarity. Material removal rate (MRR) and surface roughness (Ra) are the output responses. Taguchi-Grey relational approach is adopted for DOE and optimization analysis. Observations show GV and FP most significant factors for MRR and Ra both. Optimal values of the parameters based on grey relational include Ton=5, I= 5A, GV=40V, N=40 RPM and FP=0.25 kg/cm². Comparison of confirmation experiments based on orthogonal array and predicted grey relational array shows 2.23 times improvement in surface finish and 3.3 times decrease in MRR.
- Chen et al. [20] uses micro-reciprocated Wire Electro discharge Turning (WEDT) for the fabrication of micro-rotating structure for material like cemented carbide K15 that are very difficult to machine or turn with conventional processes. CCD of RSM and ANOVA techniques are used to design and analyze the significance of the factors like open voltage (U), discharge capacitance (C) and rotational rate (R) on the MRR and surface roughness (Ra). Multiple cutting Strategies are employed and experiment is performed for rough (RM), semi-finish (SFM) and finish machining (FM). Observations show increase of MRR with increase in U, C and R initially, but at large value of U MRR becomes stable and at large values of C MRR tend to fall. Ra increases with increase of U and C but decreases with increase of R. Using desirability function, 3 sets of optimal parameters are chosen for Multi cutting strategy. Confirmation Experiments shows an error of 1.75~7.76 % for MRR and 2.77~8.59 % for SR. Finally a micro-probe balloon structure of 987 μm diameter is fabricated with the obtained optimal parameters with high dimensional accuracy and good surface finish of 0.435 μm Ra.

- Balamurali et al [21] perform the CWEDT for parametric optimization for MRR and Ra using the Taguchi Robust design. Gap voltage (GV), Pulse ON time (Ton), Pulse OFF time (Toff), Wire feed (N), Rotational rate (R) are chosen the parameters and material used is stainless steel (SS316 grade). Max MRR achieved is $2.189 \text{ mm}^3/\text{min}$ at $R=500 \text{ rpm}$, which found to be most significant factor for MRR; Ton shows the least significant effect. Ra is mostly influenced by Ton in the inverse proportionality and recorded $\text{Ra}=2.089 \mu\text{m}$ at $\text{Ton}=8 \mu\text{s}$. Ra is directly proportional with GV with less significant than Ton. Rotational speed (R) least effect the Ra.
- Srivastav et al [22] employs WEDT on newly developed hybrid metal matrix composite (MMC) of aluminum (A359/B4C/Al₂O₃) and investigated the surface integrity (Ra, Rq, Rz), surface morphology, residual stress on machined surface and micro-hardness variation with the rotational speed (N). Dull appearance of the tuned surface with no cracks or deformities attributed due to the thermal effects on the resoldified layer is observed. Better surfaces are reported as Surface integrity parameters Ra, Rq and Rz shows a decreasing trend with the increase in the rotational speed with 22.58, 19.78 and 16.16 % respectively up to 600 rpm. Reason stated was decrease in the discharge energy per unit time for the same spark zone. MRR shows decreasing trend with the increase in the rotational speed with max MRR = $33.07 \text{ mm}^3/\text{min}$ at $N=200 \text{ rpm}$. 2D & 3D micro structural visuals shows the decrease of scales, porosity and voids with increase rotational speed. Micro-hardness increases and Residual stresses decrease with increase in rotational speed due to reduction in HAZ. This study states the decrease in effective spark in case of WEDT as the major differential factor between WEDM and WEDT.

Table 2.1 Literature Review

Author & Year	Title	Inference	Literature Type
R.Magabe, N.Sharma, K.Gupta, J.P. Davim; 2019	Modeling and optimization of Wire-EDM parameters for machining of Ni55.8Ti shape memory alloy using hybrid approach of Taguchi and NSGA-II	Modelling and parametric optimization shows better surface quality and increased MRR. Feasibility of new Hybrid approach is also stated.	Parametric optimization
Jun Qu & Shih, 2002	Development of the Cylindrical Wire Electrical Discharge Machining Process, Part 1: Concept, Design, and Material Removal Rate	CWEDT setup fabrication is done and Comparison of WEDM & WEDT on MRR basis	Setup Fabrication
Jun Qu & Shih, 2002	Development of the Cylindrical Wire Electrical Discharge Machining Process, Part 2: Surface Integrity and Roundness	Modelling of surface roughness and Roundness. Good surface finish shows reduced MRR. Individual optimization is done for MRR and Surface finish.	Parameters modelling and study
Haddad, M. Tajik,A.Fadaei Tehrani et al., 2009	An experimental investigation of cylindrical wire electrical discharge turning process using Taguchi approach	Full Factorial is employed for parametric optimization for MRR, Surface roughness and roundness. Better conditions of surface are achieved with increased MRR.	Parameter optimization using full factorial
Haddad, Alihoseini 2009	An experimental investigation of cylindrical wire electrical discharge turning process	Surface roughness, micro-hardness and surface analysis shows dependency on discharge energy. EDAX shows deposition of Cu and Zn on machined samples.	Surface Microstructure Investigation w.r.t discharge energy

Haddad et al., 2007	Material removal rate (MRR) study in the cylindrical wire electrical discharge turning (CWEDT) process	Parametric Optimization using RSM for Recast layer is done. Surface topography shows less craters and voids with increase of rotational speed.	Parametric optimization
Mohammadi et al., 2014	Investigation on the effects of ultrasonic vibration on material removal rate and surface roughness in wire electrical discharge turning	US-vibration and Power shows significant effects on MRR, Surface roughness. Low power with US-vibrations shows better quality and productivity.	New parameter (Involvement of New parameter US-Vibrations and its effects.)
Mohammadi et al., 2014	Investigation of ultrasonic-assisted wire electrical discharge turning based on single discharge analysis	US-Vibration increases the MRR as length of crater decreases due to which more energy per discharge.	New approach
Mohammadi, Fadaei et al., 2016	Modeling and optimization of the process parameters in ultrasonic-assisted wire electrical discharge turning	CCD is employed to study influence of lateral US-vibrations. US-Vibration shows insignificant Effect on surface finish and roundness	Parametric optimization
Janardhan, G.L.Samuel , 2010	Pulse train data analysis to investigate the effect of machining parameters on the performance of wire electro discharge turning (WEDT) process.	MRR, Surface finish and Roundness is studied on basis of type, delay time and flux of Discharge.	Pulse train data analysis (Discharge analaysis))
A.Giridharan & G.L.Samuel, 2018	Investigation into erosion rate of AISI 4340 steel during wire electrical discharge turning process	New Model is Proposed for erosion rate calculation. Experiments show the validation of proposed model.	New Model
Y.Sun, Y.Gong etal, 2017	Experimental study on surface characteristics and improvement of microelectrode machined by low speed wire electrical	Micro-electrode of 90µm dia. is fabricated using Multi-cutting strategy and surface	Fabrication of micro-electrode

	discharge turning	finish of $0.59\mu \text{ Ra}$ is achieved at Fine Cut.	
Y.Sun, Y.Gong, et al., 2017	Experimental study on the microelectrodes fabrication using low speed wire electrical discharge turning (LS-WEDT) combined with multiple cutting strategy	Bending and Breaking of the micro-electrode is analyzed. Discharge Energy and flushing shows significant effects. Micro-cutting tools are fabricated.	Analysis on Micro-structures
V.Gohil, Y.M. Puri , 2018	Optimization of Electrical Discharge Turning Process using Taguchi-Grey Relational Approach	Significant Effects of Gap voltage and Flushing on MRR and surface finish are shown.	Parametric optimization using Taguchi-grey function.
X.Chen, Z. Wang et al., 2018	Micro reciprocated wire-EDM of micro-rotating structure combined multi-cutting strategy	Micro-probe structure is fabricated using CCD technique and desirability is employed that shows improvisation in the results.	Fabrication of Micro-probe structure
D.Balamurali, K.Manigandan, V.Sridhar, 2015	Analysis of the Effect of Machining Parameters on Wire Electrical Discharge Turning of Stainless Steel	Parametric optimization using Taguchi. Significant importance of Pulse ON time is justified.	Parameter optimization using Taguchi
A.K. Srivastav, A. Nag et al., 2019	Surface integrity in wire-EDM tangential turning of in situ hybrid metal matrix composite A359/B4C/Al ₂ O ₃	WEDT of composite (MMC) is done and Surface analysis shows the importance of Spindle rotational speed.	New material (MMC)
H.G. Dhake and G.L. Samuel, 2012	Machining of axi-symmetric forms and helical profiles on cylindrical workpiece using wire cut EDM	Geometrical deviations are calculated for complex profiles.	Complex profiles generation

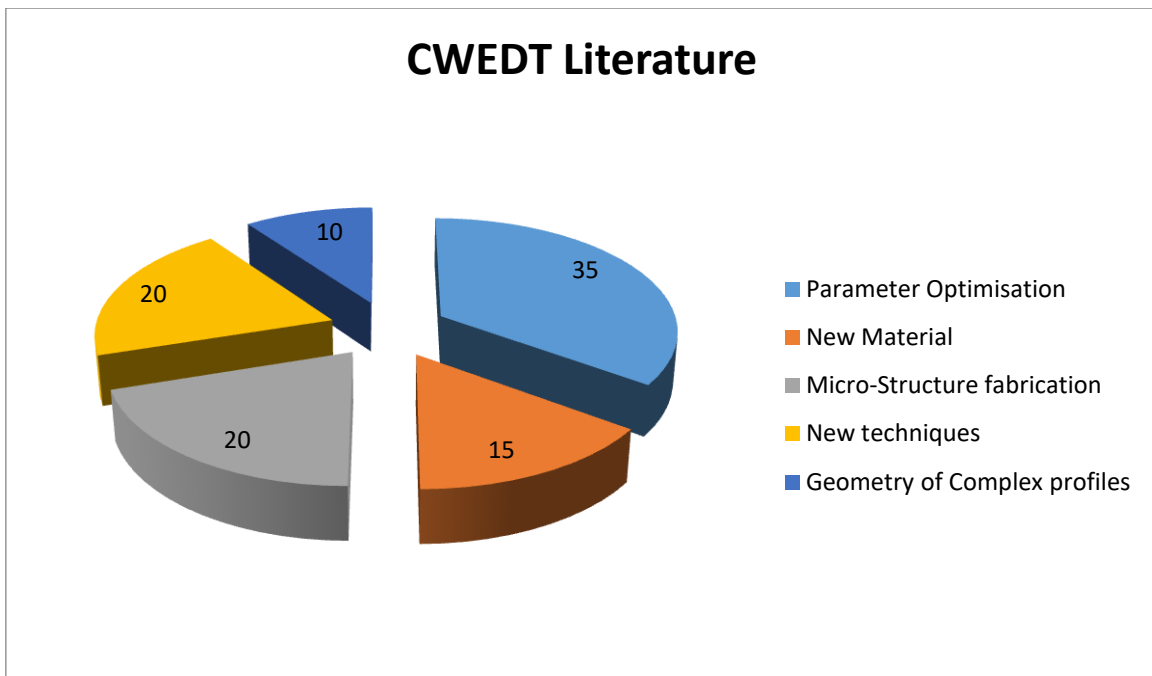


Fig. 2.1 CWEDT Literature

2.2 Critical Research Gap

Literature on CWEDT is studied thoroughly with some literature of EDM and WEDM. Fig 2.1 shows the pie chart with the literature contribution of different type. As shown parametric optimization for better output responses are the most applied in the studied literature with 35 %. The New techniques that include 2D crater measurement for erosion, Surface effects on single discharge basis and the application of ultrasonic (US) vibrations to the wire of WEDT have a share of 20 % in the studied literature. Micro-structures like probes, micro-electrodes and other cutting tools fabrication work as shown in chart contribute 20% in the literature. It is found only 10 % work has been reported on geometries and measurement of the complex profiles machined by CWEDT. However Surface Integrity, microstructural along with the geometric deviation of the geometries analysis together contributes less than 5% in the studied literature. It is also noticed that no research has been carried out for the multi-objective optimization for different geometries of the complex shaped profile. Hence, Objective and motivation of the present research work is gained through these literature gaps.

2.3 Motivation and Objective

With above studied literature and identifying the literature gap, an attempt has been made to quantify the process capability of the cylindrical wire electrical discharge turning (CWEDT) by the experimental analysis for the investigating the 3D complex profile structure fabricated under the influence of different parameters. Motivation during the whole research is taken from the research gaps and carried insight for new findings & development for the machining of micro and macro level complex profiles used in industries. Due to extensive use of superalloys in modern industries, present research is also look into the machinability of such alloys.

The Objectives of the present study are:

- To make a complex profile using the CWEDT
- To investigate machining rate and surface Integrity of the different geometries while making the complete profile.
- To investigate the roundness of the profile made by CWEDT.
- To investigate the dimensional error in CWEDT of complex profiles.
- To perform Multi-Objective response optimization for spherical, cylindrical and taper turning.
- To perform Multi-Objective response optimization for 3D complex profile structure fabricated by CWEDT.

Chapter 3 - Methodology and Experimentation

In the following chapter discussions are made on the Equipment and work piece material, machine parameters, output responses and their significance, Ideal profile of the 3D structure fabricated in the project, mathematical modelling of MRR, methodology for design of experiments, the desirability function for the optimization of the process under the influence of process parameters and the experimentation recorded values.

3.1 Experimental setup



Fig. 3.1 CWEDT Setup

Experiments are conducted on 3-axis Electronica Maxicut 374 flushing type wire electrical discharge machine (WEDM). The Conventional WEDM setup employed in the research made to hybridize by mounting of the rotary spindle system in order to rotate the work piece. Rotating workpiece continuously been flushed by the deionized water from the upper and lower nozzles in order to generation of the spark. Spindle is the key part of the system. Proper design and alignment of the spindle to the motor housing is utmost necessary for maintain the

accuracy and precision of the machining. Safety of the experiment also lays side by the spindle flexibility and zero-error. A spindle must meet design requirement like Flexibility, Accuracy, Power connection and Corrosion Resistance for the proper operation. Figure 3.1 shows the rotary spindle system with the microprocessor that controls the spindle speed and frequency. Also, Figure 3.1 depicts the CWEDT setup with all necessary labeling.

3.2 Workpiece Material and Complex Geometries

Titanium grade 12 is used as the work material in CWEDT. Round bar of 10 mm diameter with grounded and forged conditions is employed. Due to its high melting temp, high hardness and toughness, it makes it suitable in field of research to deploy it inorder to generate shapes and geometries and obtain the data. Exotic materials and super alloys like Titanium, nickel alloys, tungsten alloys etc. very difficult machine by conventional processes. EDM and WEDM enables the cutting and machining of such alloys, Currently used work material Ti grade 12 have many applications including aerospace, bio medical, heat exchangers, marine , chemical industries, automobile industries and tool industries. Fig 3.2 depicts the EPMA graph of the Ti grade 12 with various constituents beside pure titanium like nickel, zinc, chromium.

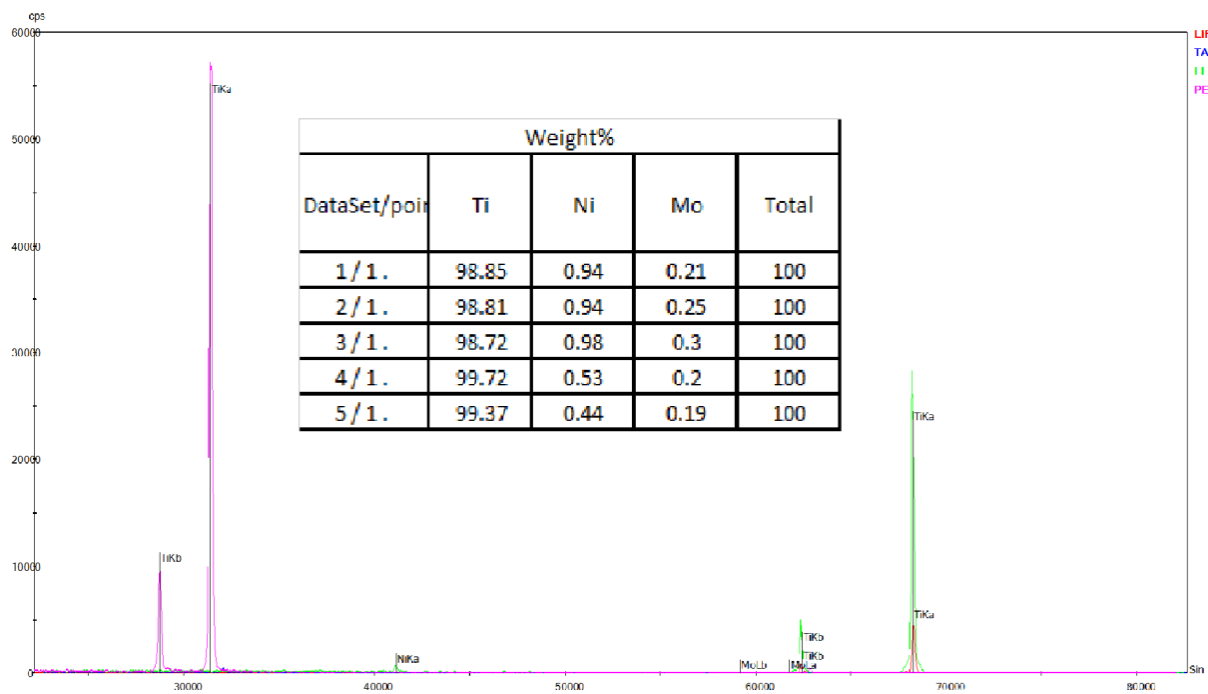


Fig.3.2 EPMA graph of work material

3.2.1 Analysis and Modelling of the 3D Probe Structure

Design of the fabricate part is taken from the reinshaw probe styl reference technical data book; Fig 3.3 shows the design taken as reference. CWEDT of work material taking above reference design is done. Fig 3.4 shows the actual probe fabricated on CWEDT. Complex shaped profile of the design consist of three geometries namely Spherical, cylindrical and taper. Thus, in the present study, analysis of spherical turning, cylindrical turning and taper turning is done w.r.t MRR and Ra under the influence of various combination of the parameters. Roundness of the spherical turned part is also measured for various sets of experiments. Fig 3.5 shows the various sections of the probe.

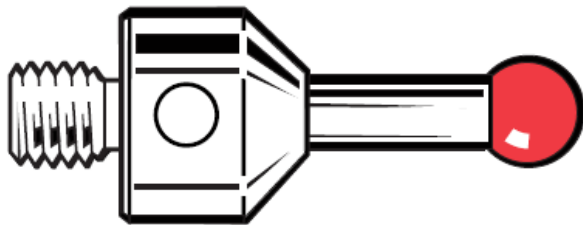


Fig. 3.3 Ideal Reference probe



Fig. 3.4 Actual CWEDT probe

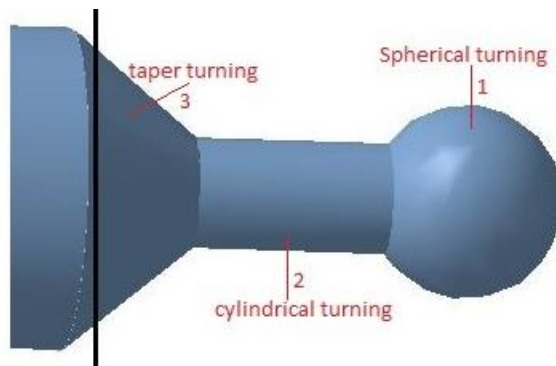


Fig. 3.5 Types of CWEDT

Mathematical modelling of the 3D probe is done for MRR and MRR equations are derived in the following section.

In order to calculate the MRR, Volume of each geometry of the 3D probe shaped structure needs to be find. For that whole geometry is divided into three parts namely spherical,

cylindrical and tapered. Following Steps are taken to find out the MRR of each geometrical shape:-

- Derivation of the volume expression of each geometrical part i.e. spherical, cylindrical and tapered.
 - Calculating the eroded volume by subtracting the volume of geometry from the original dimension of the workpiece enveloping it.
 - Using the formula
$$MRR = \frac{\text{Eroded volume of the material}}{\text{Time taken}}$$

Step 1- Deriving expressions for the Volume of Geometries

(i) Volume of Spherical part (V_1):-

$$V = \int_d^{d+h} \pi r^2 \, dy$$

$$V = \pi \int_d^{d+h} (R^2 - y^2) dy$$

$$V = \pi [R^2 y - \frac{y^3}{3}] \frac{d+h}{d}$$

$$\left[V = \pi \left[R^2 - d^2 - hd - \frac{h^2}{3} \right] h \right] \dots \dots \dots \quad ①$$

$$a = \sqrt{R^2 - d^2}$$

$$h + d = R$$

$$a^2 = R^2 - (R - h)^2 = 2Rh - h^2$$

$$\left\{ R = \frac{a^2 + h^2}{2h} \right\} \dots \dots \dots \textcircled{2}$$

$$d = R - h = \frac{a^2 + h^2}{2h} - h = \frac{a^2 + h^2 - 2h^2}{2h}$$

$$\left\{ d = \frac{a^2 - h^2}{2h} \right\} \dots \dots \dots \quad (3)$$

Putting value of R and d from ② and ③ into ①

$$V = \pi h \left[\left(\frac{a^2 + h^2}{2h} \right)^2 - \left(\frac{a^2 - h^2}{2h} \right)^2 - h \left(\frac{a^2 - h^2}{2h} \right) - \frac{h^2}{3} \right]$$

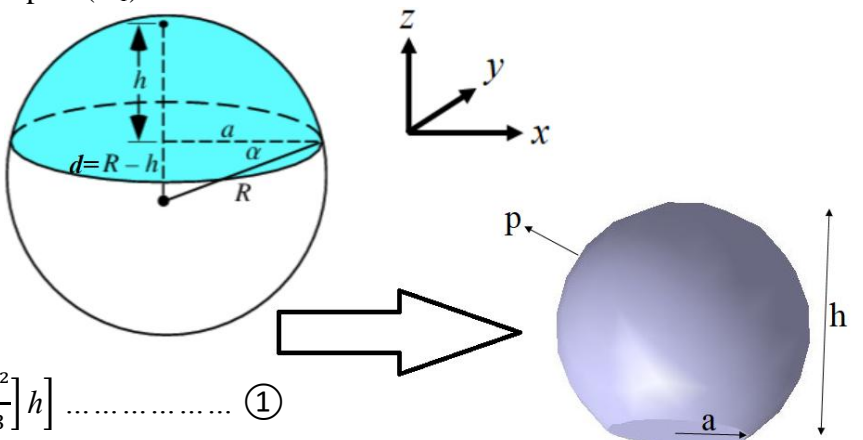


Fig. 3.12

$$V = \pi h \left[\frac{6a^2 - 3a^2 + 3h^2 - 2h^2}{6} \right]$$

(ii) Volume of Cylindrical part (V_2):-

$$[V_2 = \pi r^2 H] \dots \beta$$

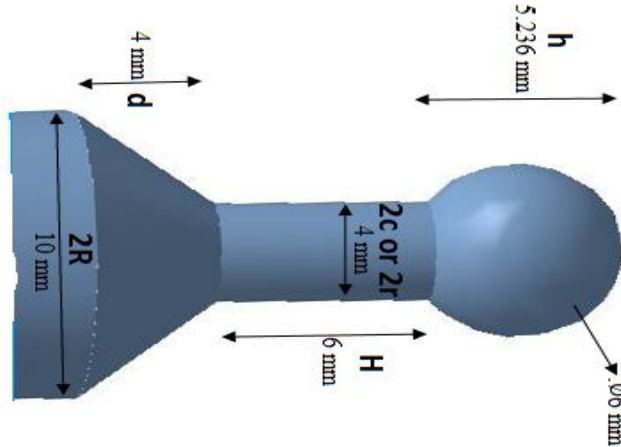


Fig.3.7 Geometry of Tapered and Cylindrical part

(iii) Volume of Tapered part (V_3):-

$$\left[V_3 = \frac{\pi h}{3} (R^2 + r^2 + Rr) \right] \dots \gamma$$

Step 2- Calculating the Eroded Volume in each turning operation

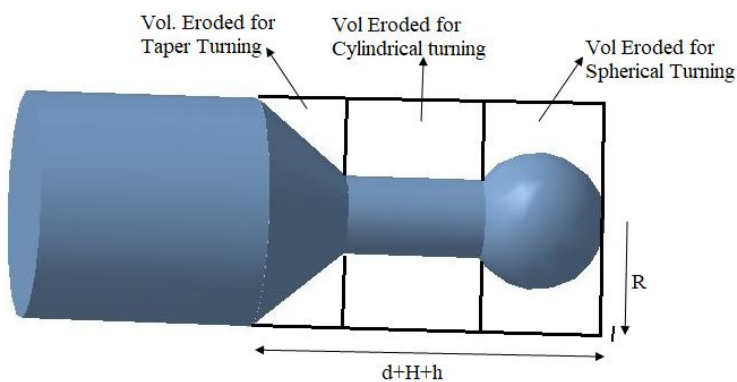


Fig. 3.8 Calculation of Eroded Volume

- Eroded Vol. during Spherical Turning= V_{11}

$$V_{11} = \pi R^2 h - V_1$$

- Eroded Vol. during Cylindrical Turning= V_{22}

$$V_{22} = \pi R^2 H - V_2$$

- Eroded Vol. during Taper Turning= V_{33}

$$V_{33} = \pi R^2 d - V_3$$

Step 3- Calculating the MRR for each geometrical shape

While performing the experiments, time for each turning is recorded as t_1 , t_2 and t_3 . MRR is calculated using above find expressions and putting in the below given MRR formula.

$$\left[\text{MRR} = \frac{\text{Eroded volume of the material}}{\text{Time taken}} \right] \frac{\text{mm}^3}{\text{sec}}$$

- MRR for Spherical Turning: $\text{MRR}_1 = \frac{V_{11}}{t_1}$
- MRR for cylindrical Turning: $\text{MRR}_2 = \frac{V_{22}}{t_2}$
- MRR for Taper Turning: $\text{MRR}_1 = \frac{V_{11}}{t_1}$

3.3 Process Parameters

WEDM in terms of the process parameters is one of the most complex machining setup. Due to large number of parameters it is very difficult to control its productivity. Process parameters includes pulse-on time, pulse off time, peak current, sensitivity, gap voltage, flushing power, wire tension, wire feed, types of wire, wire thickness, type of dielectric, discharge capacitance and dielectric conductivity . By adding the rotary spindle system, along with above listed factors spindle rotation rate (N) as anew factor. Fig 3.9 show the process parameters of WEDMT

Some important parameters are:-

Pulse-ON time (Ton): - It signifies the duration of the spark generated. More pulse on time more discharge energy supplied to the sample and hence higher machining rate. Initially MRR increase but after sometime MRR decreases and surface becomes dull.

Pulse-OFF time (Toff):- it signifies the duration between the two sparks. When pulse off time is very less then there is more time for energy input and machining rate increase but with continuous lower pulse off, debris and molten material are not properly flushed and thus quality of the surface deteriorates.

Gap Voltage (GV):- It is the potential barrier needed for ionization of the dielectric between the work gaps. It controls the gap between the tool and workpiece inorder to change the discharge energy for the spark. Lower values will cause more MRR as the distance between the electrodes decreases. surfaces quality deteriorates as GV decreases.

Flushing Power (FP):- Machining rate and surface produces with high flushing power are found better. Flushing of the dielectric acts like a medium for circuit completion. Flushing removes the debris accumulate in the spark zone. It also reduces the HAZ. Less flushing may lead to wire breakage due to generation of large amount of heat and pressure.

Wire material and diameter: - usually wire material used is zinc coated brass of 250-500 μm diameter. Large no of array of wire material are available for different work materials like molybdenum, tungsten, vanadium coated. Wire thickness increases the kerf and thus crater size increases.

Wire Feed (WF): - Wire feed increases the machining rate Wire feed is directly proportional to the contact time of the wire in the spark zone.

Wire Tension (WT):- bending and vibrations of the wire during the machining are two common defects occurs due to the less wire tension. Sufficient wire tension is required to avoid and vibration and breakage. Too large or too low wire tension is undesirable.

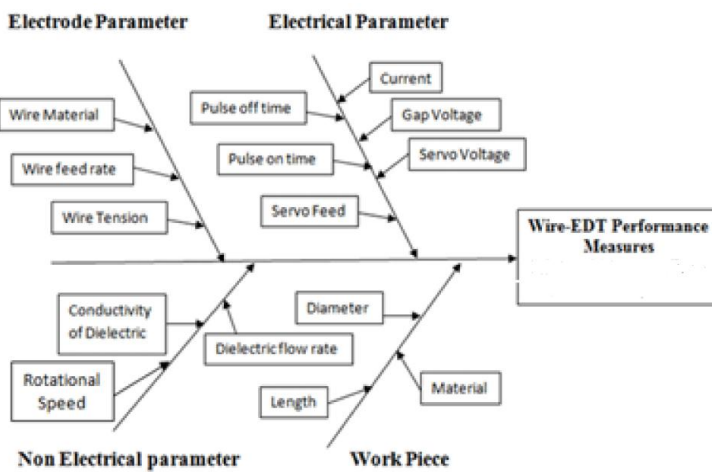


Fig.3.9 CWEDT parameters [27]

In the present research pulse-off time (Toff), gap voltage (GV) and rotational rate (N) are selected as the process parameters and suitable methodology is used to design the combinations for performing the experiments. Fig 3.10 shows the parameters and their levels used.

Parameter	Level 1	Level 2	Level 3
Pulse-ON time (Ton) μ s	70	130	190
Gap Voltage (GV) V	30	40	50
Spindle Speed(N) rpm	200	400	600

Fig.3.10 Parameters and their levels

3.4 Design of Experiment and Analysis Methodology

Analysis of the parameters and investigation their influence on the output responses is all done in Minitab software @18.

3.4.1 Response surface methodology (RSM)

Response surface methodology (RSM) is extensively used in the present research work for design of experiments (DOE) using the box beckon technology and Table of Analysis of variance (ANOVA) regressions equations are generated using the RSM.

Designing of experiments allow us to analysis the influence of input on the output, interactions and even quadratic effects, thus allow to generate the (local) shape of the surface that output govern, thus in this way this technique earns its name as Response surface Methodology (RSM). RSM is a mathematical and statistical technique used for modelling and analysis of the objective problem that is under the influence of numbers of variables or parameters. Relationship between the input parameters and output response is established and contour plots are generated to study the dependency and interaction between parameters and output responses.

Fig 3.11 shows the RSM methodology

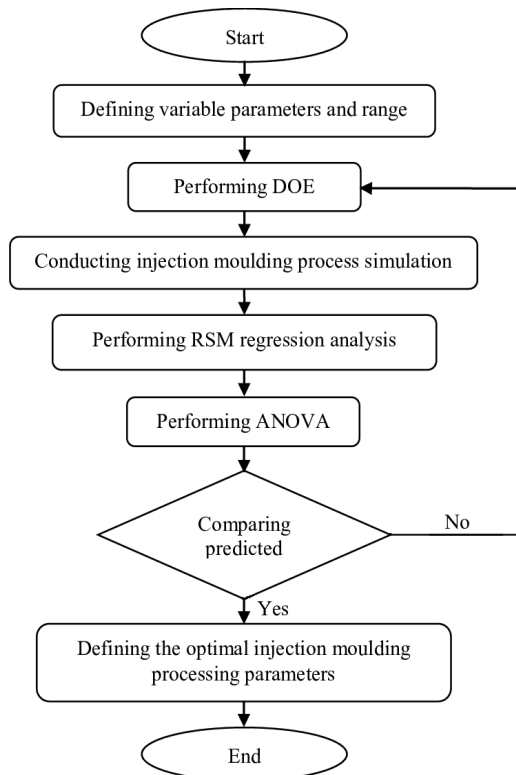


Fig.3.11 RSM Methodology

RSM involves two design techniques namely Box-Wilson central composite designs (CCD) and Box-Behnken designs (BBD)

Box-Behnken designs (BBD) is employed in the present work for the experimentation design. BBD does not contain any factorial or mixed factorial designs rather it is an independent quadratic design. In BBD treated combinations are kept at the midpoint of the edges and at the center of the cubical process space. BBD designs require three levels of each factor. Fig 3.12 shows the BBD space for 3 factors. For three factors BBD offer certain advantage than CCD by proving less n of runs, however when factor increases it is suggested to use CCD of RSM.

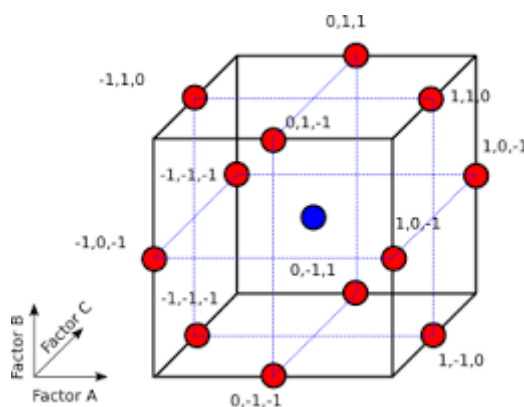


Fig.3.12 Box-Behnken Design cubical space

Pulse-off time (Toff), gap voltage (GV) and rotational rate (N) are taken as three factors in present study with three levels as listed in Fig 3.10

Table 1 shows the design of experiment via 15 different combinations.

3.4.2 Response Optimization (Desirability function)

Response surface optimizer in RSM is used for multi-objective and multi-varient optimization in order to predict the desirable output response with their nature for the productivity of the process. Desirability function involve three conditions viz. *Maximize*, *Minimize* and *Target*.

In present study, MRR is selected for maximize condition and Ra and roundness are selected for the minimize conditions.

Minitab calculates the individual desirability for each response and then weight them all according to the conditions we have assign them. Finally these all values are combined to get the composite or overall desirability for the multi-objective response optimization and optimization plot is generated.

Optimization plot generated shows how different settings affect the predicted response for a stored model

3.5 Experimentation

According to the above discussed DOE 15 experiments are performed with different set of combination and values are recorded for output response parameters for each of the geometry turned i.e. Spherical, cylindrical and tapered

Table 3.1 shows DOE table with 15 sets of experiment. All the experiments are well performed and time for each geometry machining is noted done. Observations, calculations and analysis of obtained response data is discussed thoroughly in the next proceeding chapter 4 Result and discussions.

Table 3.1 DOE Table

StdOrder	RunOrder	PtType	Blocks	A- Toff (μs)	B-GV (V)	C-N (rpm)
11	1	2	1	130	30	600
3	2	2	1	70	50	400
7	3	2	1	70	40	600
4	4	2	1	190	50	400
15	5	0	1	130	40	400
8	6	2	1	190	40	600
10	7	2	1	130	50	200
14	8	0	1	130	40	400
13	9	0	1	130	40	400
12	10	2	1	130	50	600
9	11	2	1	130	30	200
1	12	2	1	70	30	400
2	13	2	1	190	30	400
6	14	2	1	190	40	200
5	15	2	1	70	40	200

3.6 Measurement of Response parameters

Productivity of any process is measured in terms of machining rate and for that Material Removal rate (MRR) is chosen as an output response. MRR formula derivation is done in section 3.2 using mathematical modelling. (Refer equations α , β , γ in section 3.2) Surface integrity describes the metallurgical, topological and mechanical conditions of the surface. WEDM surfaces are much complicated for that Surface integrity parameter Ra i.e. Mean arithmetic roughness or center line average roughness (MAR or CLA) is also recorded for surface quality analysis. Surface Roughness Ra is measured using optical microscope shown in Figure 3.13

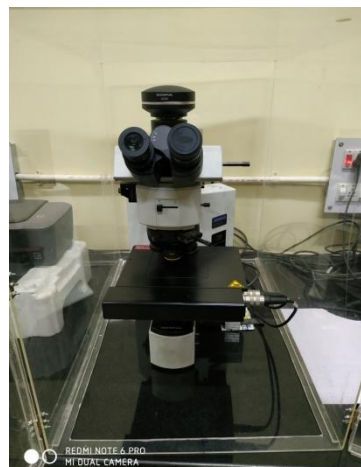


Fig. 3.13 Optical microscope

Roundness is simply the resemblance of the body mathematically with the ideal circle. Measuring the diameter is not same as measuring roundness. Roundness depicts the ratio of the inscribed and the circumscribed circles as per ISO. Roundness measures the mean circle that is bounded between the peak and valley circle as shown in Fig. 3.14; Roundness simply signifies the error that needs to be minimized. In the present study Mitutoyo RA-116 Roundness Tester is used for measuring the roundness of geometry made by spherical turning. Roundness tester is shown in Fig. 3.15

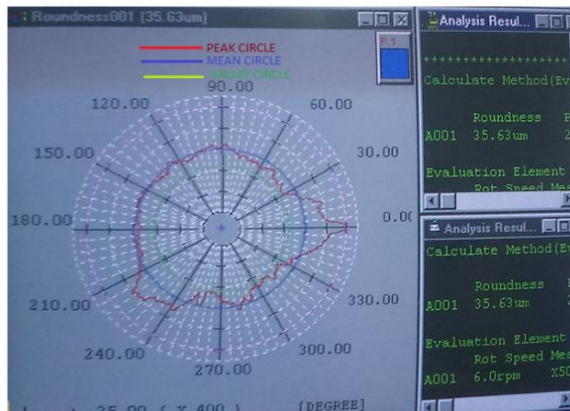


Fig. 3.14 Roundness Circles



Fig. 3.15 Mitutoyo Roundness Tester

Geometrical accuracy is one of the important considerations while making complex profiles or form generation. Any departure from the ideal shape due to machine or human error will affect the productivity of the process. Dimensional error (Δe) and Roundness (R) are other output response selected for measurement of the profile and its surface topography.

Chapter 4 Results and Discussion

Fabrication of 3D complex profile is done experimentally using the Box-Behnken technique of Response surface methodology (RSM) and analysis is done using ANOVA. Regression equations are obtained using RSM. Finally, Multi-Objective Optimization is done for each geometrical feature and also for complete profile.

Keywords: *CWEDT, WEDM, MRR, Ra, R, Pulse OFF Time (Toff), Gap Voltage (GV), Rotational Speed (N)*

Table 4.1 Experimentation data

StdOrder	RunOrder	PtType	Blocks	A	B	C	Roundness (μ)	MRR1	MRR2	MRR3	Ra1	Ra2	Ra3
11	1	2	1	130	30	600	28.9300	12.8135	13.9039	11.2500	2.9650	2.2000	3.200
3	2	2	1	70	50	400	41.2100	10.1000	10.8492	9.8500	1.7500	1.2400	2.000
7	3	2	1	70	40	600	30.5409	11.4100	11.9500	10.6500	2.1570	1.3200	2.756
4	4	2	1	190	50	400	35.8500	8.3170	8.2465	8.1478	1.1000	0.5760	1.230
15	5	0	1	130	40	400	35.9400	12.5772	13.7280	11.1722	2.7640	2.0476	3.175
8	6	2	1	190	40	600	28.3700	9.2524	9.0947	8.5000	1.3200	1.1000	1.540
10	7	2	1	130	50	200	58.4900	12.0535	12.4540	10.9590	2.5870	1.5780	2.985
14	8	0	1	130	40	400	35.9400	12.5772	13.7280	11.1722	2.7640	2.0476	3.175
13	9	0	1	130	40	400	35.9400	12.5772	13.7280	11.1722	2.7640	2.0476	3.175
12	10	2	1	130	50	600	31.7200	9.8000	10.5171	9.1000	1.6500	1.2000	1.850
9	11	2	1	130	30	200	54.2000	12.9670	13.9165	11.6500	3.0980	2.4500	3.200
1	12	2	1	70	30	400	38.0200	13.9320	14.7500	12.9750	3.4700	2.8700	4.540
2	13	2	1	190	30	400	34.8600	10.2500	10.9500	9.9500	2.0125	1.2800	2.436
6	14	2	1	190	40	200	47.3450	9.7500	10.4250	8.9500	1.4500	1.1950	1.600
5	15	2	1	70	40	200	61.2000	13.7500	14.2750	12.6500	3.3700	2.7650	3.760

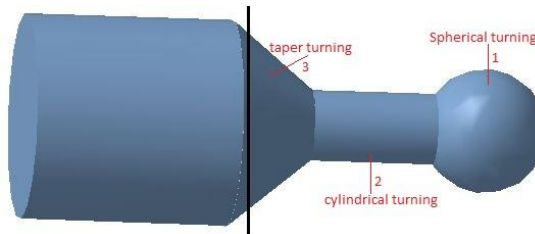


Fig. 4.1

4.1 MRR Discussion for Spherical (MRR1), cylindrical (MRR2) and taper tuning (MRR3)

MRR is calculated using the equation α, β, γ derived in section 3.43 for each set of experiment and calculating the machining time for each geometry of the profile generated. Table 2, Table 3 and Table 4 shows ANOVA table for MRR1, MRR2 and MRR3 respectively. All tables shows that taken factors Toff, GV and N are highly significant individually but some interaction are insignificant like Toff with GV, Self-interaction of Toff, GV and N. Model summary of the ANOVA for MRR1, MRR2 and MRR3 indicates that model fits the data well as R-sq adj and R-sq (pred.) are high as desirable for better model

feasibility and predictability. Regression equations for MRR1, MRR2 and MRR3 are generated below using RSM and insignificant terms are deleted.

$$MRR1 = 8.20 + 0.0297 A + 0.305 B + 0.00501 C - 0.000388 A^2 - 0.00530 B^2 - 0.000003 C^2 + 0.000791 A \cdot B + 0.000038 A \cdot C - 0.000262 B \cdot C$$

$$MRR2 = 3.61 + 0.0813 A + 0.395 B + 0.01135 C - 0.000526 A^2 - 0.00634 B^2 - 0.000010 C^2 + 0.000499 A \cdot B + 0.000021 A \cdot C - 0.000241 B \cdot C$$

$$MRR3 = 13.15 - 0.0031 A + 0.060 B + 0.00491 C - 0.000207 A^2 - 0.00195 B^2 - 0.000006 C^2 + 0.000551 A \cdot B + 0.000032 A \cdot C - 0.000182 B \cdot C$$

Fig. 4.2, Fig. 4.3(a, b, c), Fig. 4.4 shows the Individual plots of the factors with MRR1, surface plots between factors and MRR1 and Normality plot of MRR1 respectively. Similarly Fig. 4.5, Fig. 4.6 (a, b, c), Fig. 4.7, depicts for MRR2 and Fig. 4.8, Fig. 4.9 (a, b, c), Fig. 4.10 depicts for MRR3. From the individual plots and the surface interaction plots it is shown clearly that as GV increases MRR decrease, reason for decrease in MRR can explain by the gap theory which states as the gap between the electrodes increases the energy with which spark occurring reduces and less forces are developed on workpiece surface with less penetration power, which finally decreases the MRR. With increasing value T-off initially increases the MRR and the sharply decreases continuously ; reason for Toff behavior can be stated as initially with decrease in spark interval, MRR increase as more discharge energy is penetrating the workpiece but after sometime when continuous spark occurs over long time deposition occurs over the surface which reduces the MRR. Spindle speed shows very less effect on MRR, as N increases MRR decrease as spark-workpiece contact time decreases. Normal probability distribution curve indicate data points are close to normal approximation and closely fits the predicted model.

Table 4.2

ANOVA TABLE for MRR1					
Source	DF	Adj SS	Adj MS	F-Value	P-Value
Model	9	42.7936	4.7548	47.04	0
Linear	3	32.0657	10.6886	105.74	0
A	1	16.8856	16.8856	167.05	0.012
B	1	11.7419	11.7419	116.16	0
C	1	3.4382	3.4382	34.01	0.002
Square	3	7.8753	2.6251	25.97	0.002
A*A	1	7.213	7.213	71.36	0
B*B	1	1.0363	1.0363	10.25	0.024
C*C	1	0.0713	0.0713	0.71	0.439
2-Way Int	3	2.8526	0.9509	9.41	0.017
A*B	1	0.9016	0.9016	8.92	0.031
A*C	1	0.8486	0.8486	8.4	0.034
B*C	1	1.1025	1.1025	10.91	0.021
Error	5	0.5054	0.1011		
Lack-of-F	3	0.5054	0.1685	0.18	0.6
Pure Err	2	0	0		
Total	14	43.299			
Model Summary		S	R-sq	R-sq(adj)	R-sq(pred)
		0.317934	98.83%	96.73%	81.32%

Surface Plot of MRR1 vs C, B

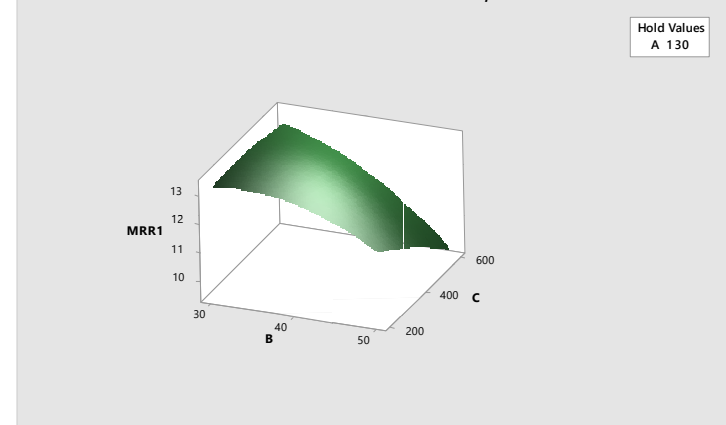


Fig. 4.3 (a)

Main Effects Plot for MRR1
Fitted Means

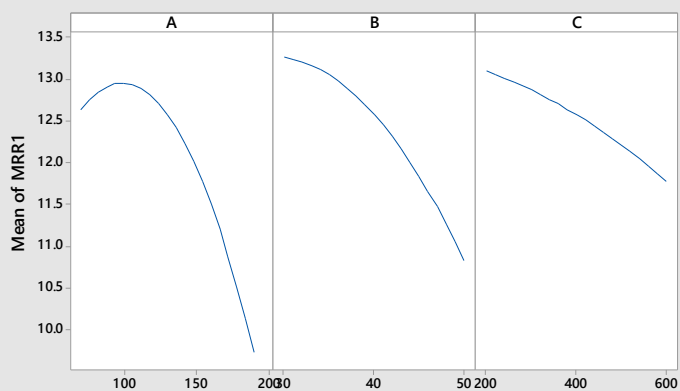


Fig. 4.2

Surface Plot of MRR1 vs C, A

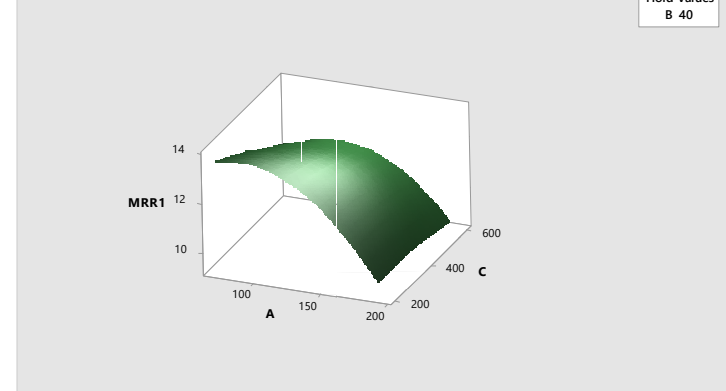


Fig. 4.3 (b)

Normal Probability Plot
(response is MRR1)

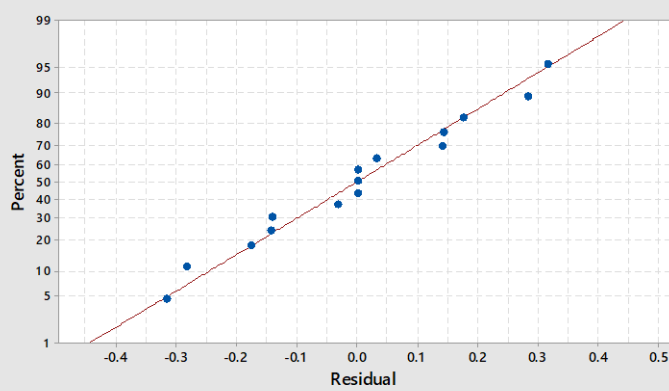


Fig. 4.4

Surface Plot of MRR1 vs B, A

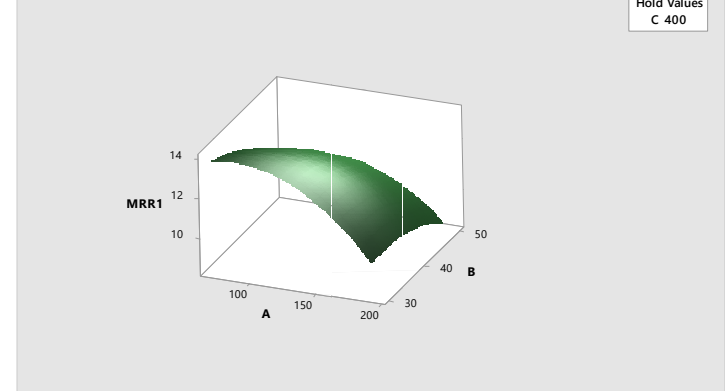


Fig. 4.3 (c)

Table 4.3

ANOVA TABLE for MRR2					
Source	DF	Adj SS	Adj MS	F-Value	P-Value
Model	9	57.6566	6.4063	42.14	0
Linear	3	41.8027	13.9342	91.65	0.009
A	1	21.4776	21.4776	141.27	0
B	1	16.3983	16.3983	107.86	0
C	1	3.9267	3.9267	25.83	0.004
Square	3	14.3224	4.7741	31.4	0.001
A*A	1	13.2645	13.2645	87.25	0
B*B	1	1.4826	1.4826	9.75	0.026
C*C	1	0.5803	0.5803	3.82	0.108
2-Way Interaction	3	1.5315	0.5105	3.36	0.113
A*B	1	0.3584	0.3584	2.36	0.185
A*C	1	0.2473	0.2473	1.63	0.258
B*C	1	0.9258	0.9258	6.09	0.057
Error	5	0.7602	0.152	0.21	0.8
Lack-of-Fit	3	0.7602	0.2534		
Pure Error	2	0	0		
Total	14	58.4168			
Model Summary		S	R-sq	R-sq(adj)	R-sq(pred)
		0.389915	98.70%	96.36%	79.18%

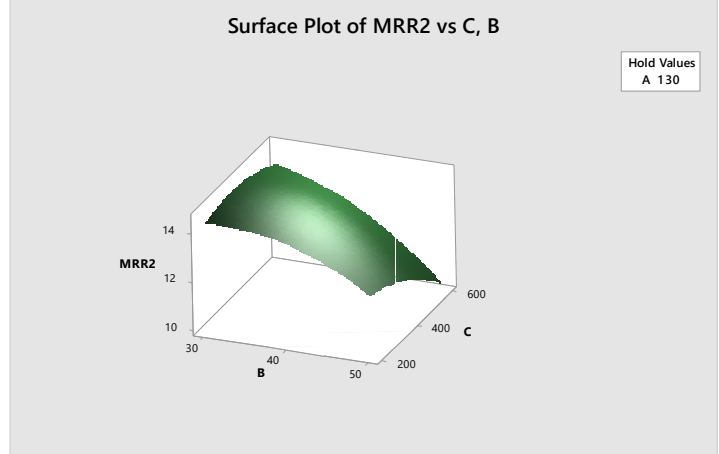


Fig. 4.6 (a)

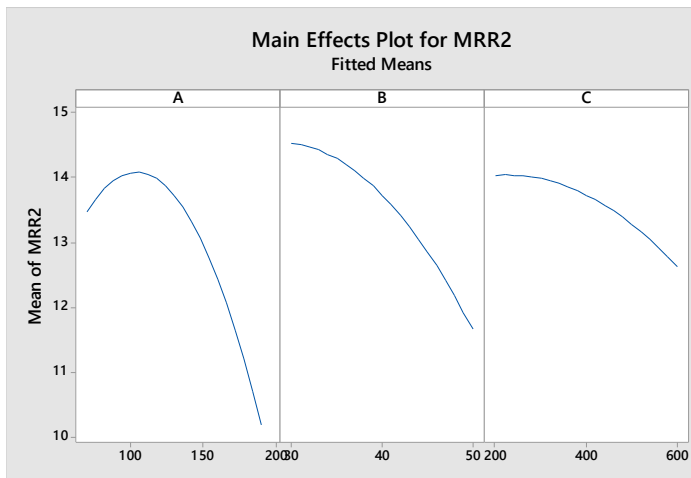


Fig. 4.5

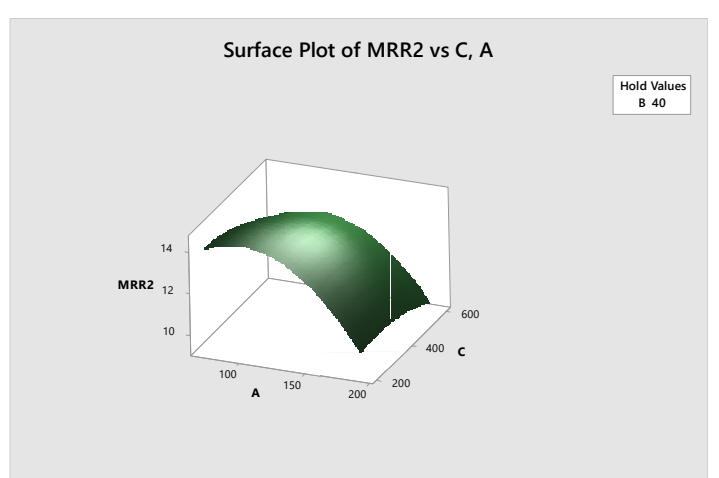


Fig. 4.6 (b)

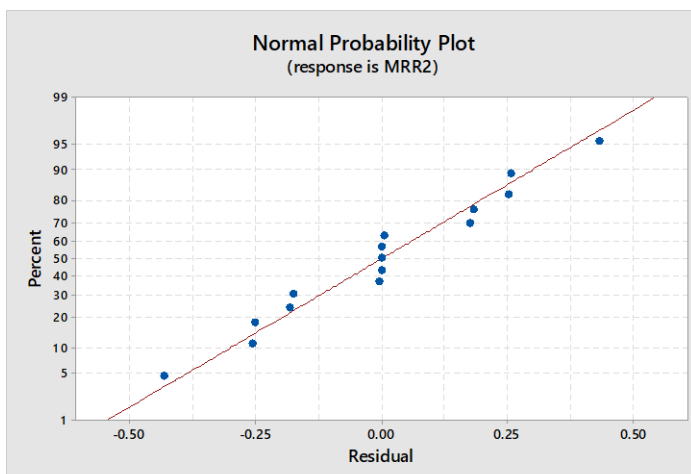


Fig. 4.7

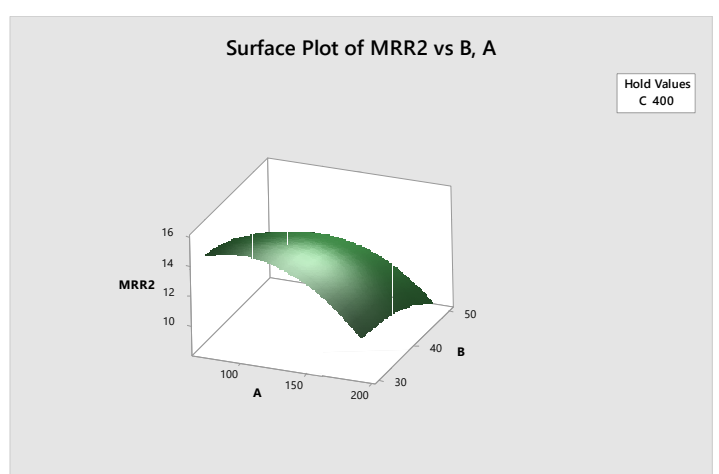


Fig. 4.6 (c)

Table 4.4

ANOVA TABLE for MRR3					
Source	DF	Adj SS	Adj MS	F-Value	P-Value
Model	9	28.1077	3.1231	22.11	0.002
Linear	3	24.2994	8.0998	57.35	0
A	1	13.9845	13.9845	99.02	0
B	1	7.543	7.543	53.41	0.001
C	1	2.7718	2.7718	19.63	0.007
Square	3	2.238	0.746	5.28	0.052
A*A	1	2.0595	2.0595	14.58	0.012
B*B	1	0.1398	0.1398	0.99	0.365
C*C	1	0.2088	0.2088	1.48	0.278
2-Way Interaction	3	1.5703	0.5234	3.71	0.096
A*B	1	0.4375	0.4375	3.1	0.139
A*C	1	0.6006	0.6006	4.25	0.094
B*C	1	0.5322	0.5322	3.77	0.11
Error	5	0.7062	0.1412	0.45	0.2
Lack-of-Fit	3	0.7062	0.2354		
Pure Error	2	0	0		
Total	14	28.8139			
Model Summary		S	R-sq	R-sq(adj)	R-sq(pred)
		0.37581	97.55%	93.14%	60.79%

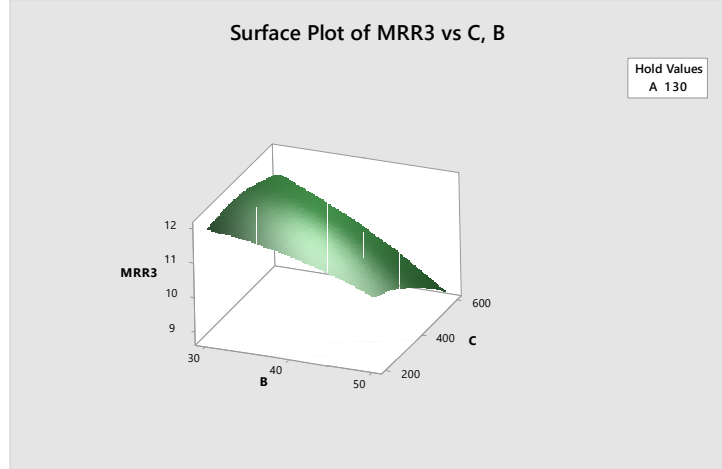


Fig. 4.9 (a)

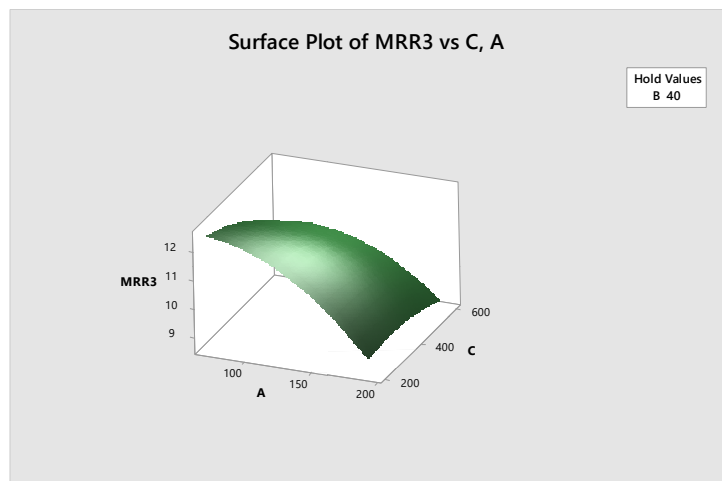


Fig. 4.9 (b)

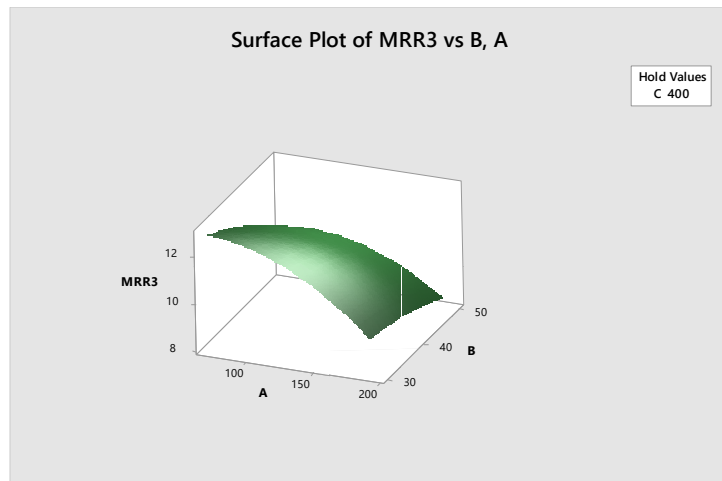


Fig. 4.9 (c)

Fig. 4.8

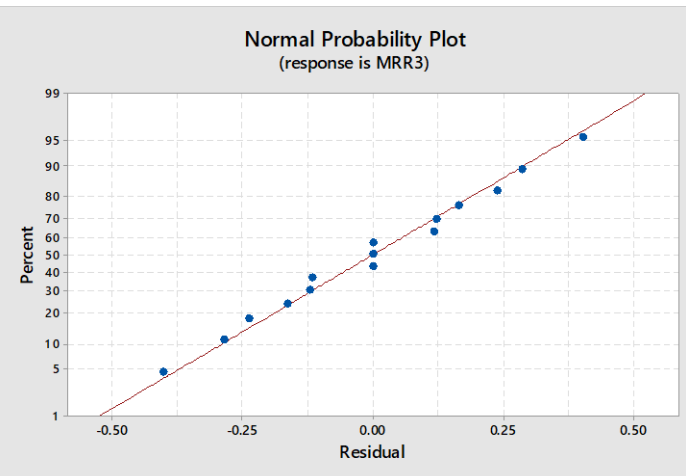
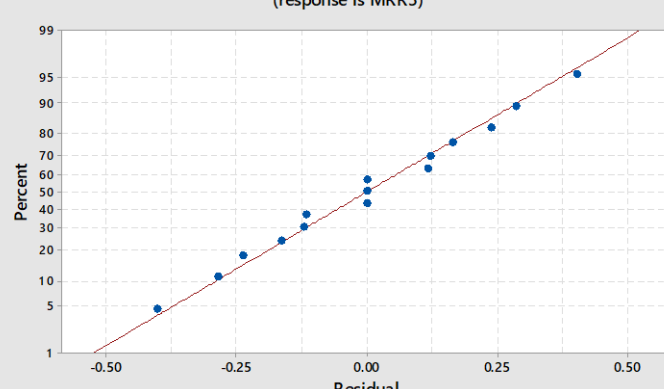


Fig. 4.10

Normal Probability Plot (response is MRR3)



4.2 Surface Roughness Discussion for Spherical, cylindrical and taper tuning (Ra1, Ra2, and Ra3)

Surface quality is one the important feature that governs the life and productivity of any product. In the present study Surface roughness is measured using the High-Definition Microscope and Ra (Arithmetic mean roughness). For a good surface finish value of Ra should be as low as possible. From Table 5, 6, 7, it can be seen that all the factors selected Toff, GV and N are all significant for Spherical (Ra1), cylindrical (Ra2) and taper tuning (Ra3). Interaction between only Toff and N shows significant among all the interactions. Model summary with R-sq (adj) of 95.12, 93.04 and 85.09 % for Ra1, Ra2, and Ra3 respectively shows that our model well fits the data along with R-sq (Pred.) in all three geometries. Ra1, Ra2, Ra3 regression equations is predicted using RSM and insignificant terms are deleted.

$$Ra1 = 3.62 + 0.01005 A + 0.0128 B + 0.00156 C - 0.000164 A^2 - 0.000901 B^2 - 0.000002 C^2 \\ + 0.000336 A*B + 0.000023 A*C - 0.000101 B*C$$

$$Ra2 = 4.55 - 0.00557 A + 0.0213 B - 0.00350 C - 0.000114 A^2 - 0.001471 B^2 - 0.000001 C^2 \\ + 0.000386 A*B + 0.000028 A*C - 0.000016 B*C$$

$$Ra3 = 4.49 - 0.0064 A + 0.010 B + 0.00678 C - 0.000141 A^2 - 0.00114 B^2 - 0.000006 C^2 \\ + 0.000556 A*B + 0.000020 A*C - 0.000142 B*C$$

Fig. 4.11, Fig. 4.12 (a, b, c), Fig. 4.13 shows the Individual plots of the factors with Ra1, surface plots between factors and Ra1 and Normality plot of Ra1 respectively. Similarly Fig. 4.14, Fig. 4.15 (a, b, c), Fig. 4.16, depicts for Ra2 and Fig. 4.17, Fig. 4.18 (a, b, c), Fig. 4.19 depicts for Ra3. It can be seen that with the Toff, GV and N all decrease Ra with their increasing value, resulting in good surface quality, It can also be seen that GV have most significant effect, followed by Toff and N influences Ra least. Surface plots shows minimum surface roughness Ra is achieved at lower Toff with low value of GV. With less Gap voltage (GV), distance between the moving wire and the workpiece decreases as a result deep impact of energy causes big size crater that leads to high values of surface roughness. With decrease in pulse-off time (Toff), continuous sparks occurs without any interval which deteriorate the surface by increase the debris deposition, HAZ and micro-cracks.. Spindle speed (N) influences the less than GV and Toff , But being significant factor N cannot be neglected as with increase in value from 200 to 600 rpm surface roughness decreases by average of 0.6 times in each of the spherical, cylindrical and taper turning. Normal probability distribution curve indicate data points are close to normal approximation and closely fits the predicted model.

Table 4.5

ANOVA TABLE for Ra1					
Source	DF	Adj SS	Adj MS	F-Value	P-Value
Model	9	8.09403	0.89934	31.37	0.001
Linear	3	6.17052	2.05684	71.74	0
A	1	2.95792	2.95792	103.17	0
B	1	2.48478	2.48478	86.67	0
C	1	0.72782	0.72782	25.39	0.004
Square	3	1.30568	0.43523	15.18	0.006
A*A	1	1.28883	1.28883	44.95	0.001
B*B	1	0.02995	0.02995	1.04	0.354
C*C	1	0.03614	0.03614	1.26	0.313
2-Way Interaction	3	0.61784	0.20595	7.18	0.029
A*B	1	0.16301	0.16301	5.69	0.063
A*C	1	0.29322	0.29322	10.23	0.024
B*C	1	0.1616	0.1616	5.64	0.064
Error	5	0.14335	0.02867	0.19	0.54
Lack-of-Fit	3	0.14335	0.04778		
Pure Error	2	0	0		
Total	14	8.23739			
Model Summary		S	R-sq	R-sq(adj)	R-sq(pred)
		0.169324	98.26%	95.13%	72.16%

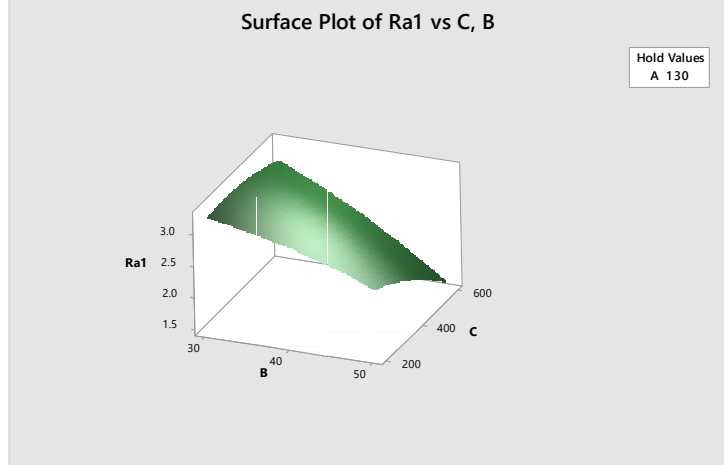


Fig. 4.12 (a)

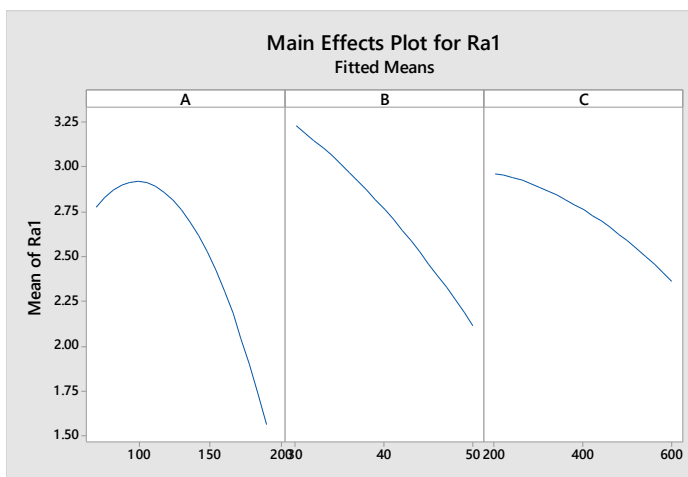


Fig. 4.11

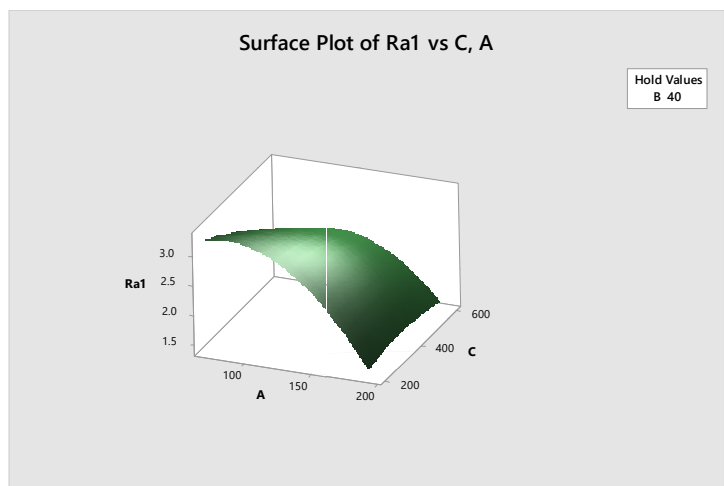


Fig. 4.12(b)

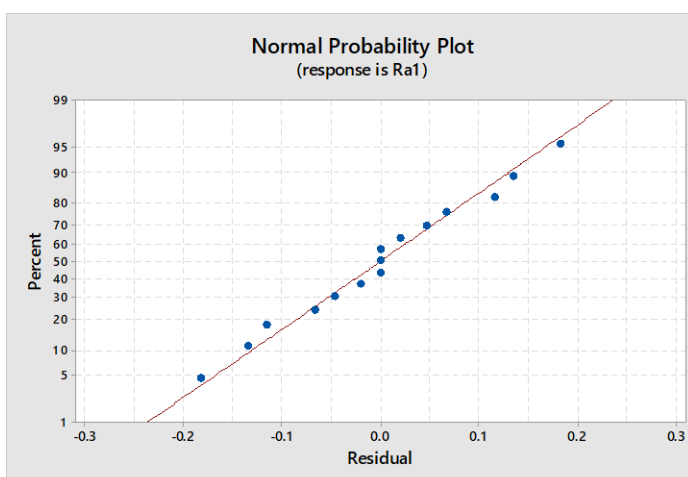


Fig. 4.13

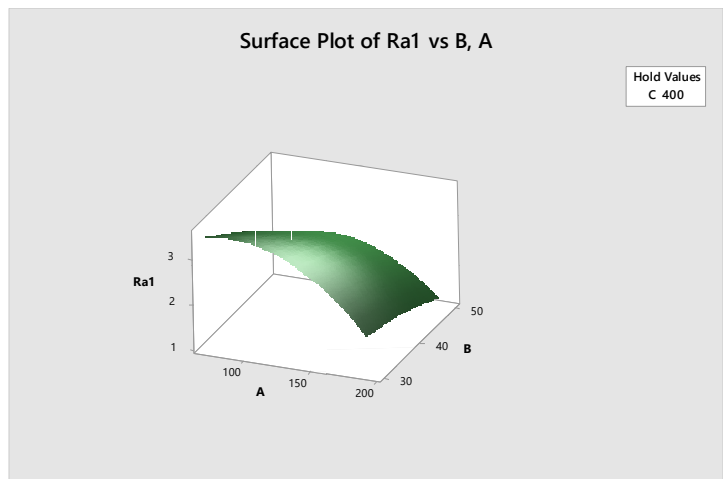


Fig. 4.12(c)

Table 4.6

ANOVA TABLE for Ra2					
Source	DF	Adj SS	Adj MS	F-Value	P-Value
Model	9	6.18465	0.68718	21.81	0.002
Linear	3	4.84307	1.61436	51.23	0.001
A	1	2.04424	2.04424	64.87	0.009
B	1	2.2113	2.2113	70.17	0
C	1	0.58753	0.58753	18.64	0.008
Square	3	0.66748	0.22249	7.06	0.03
A*A	1	0.6178	0.6178	19.61	0.007
B*B	1	0.07984	0.07984	2.53	0.172
C*C	1	0.007	0.007	0.22	0.657
2-Way Interaction	3	0.67409	0.2247	7.13	0.03
A*B	1	0.21437	0.21437	6.8	0.048
A*C	1	0.45562	0.45562	14.46	0.013
B*C	1	0.0041	0.0041	0.13	0.733
Error	5	0.15756	0.03151	0.7	0.23
Lack-of-Fit	3	0.15756	0.05252		
Pure Error	2	0	0		
Total	14	6.34221			
Model Summary		S	R-sq	R-sq(adj)	R-sq(pred)
		0.177516	97.52%	93.04%	60.25%

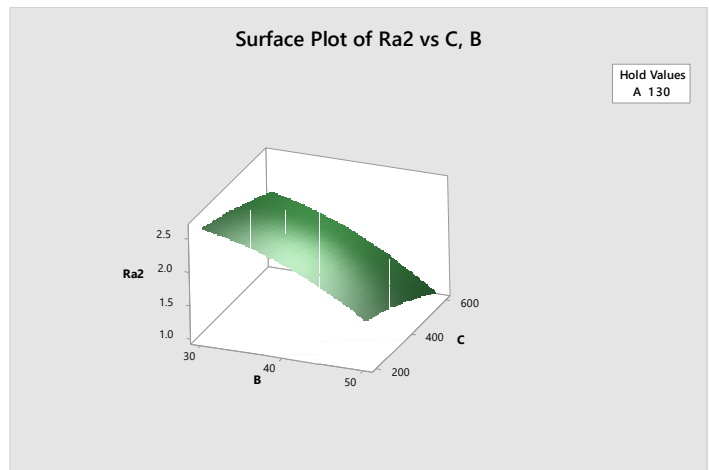


Fig. 4.15(a)

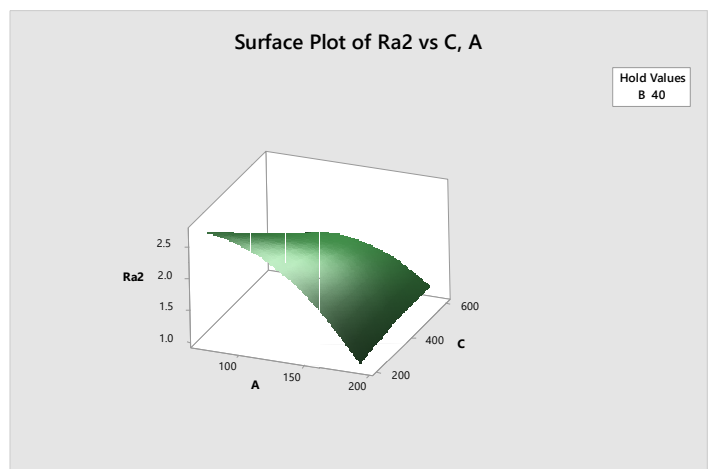


Fig. 4.15(b)

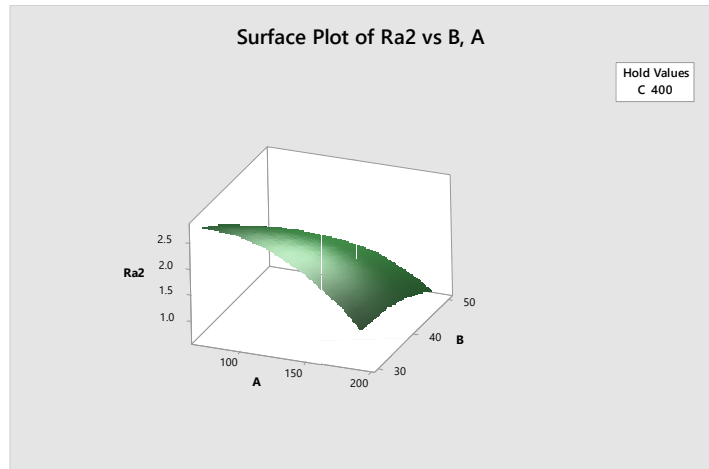


Fig. 4.15(c)

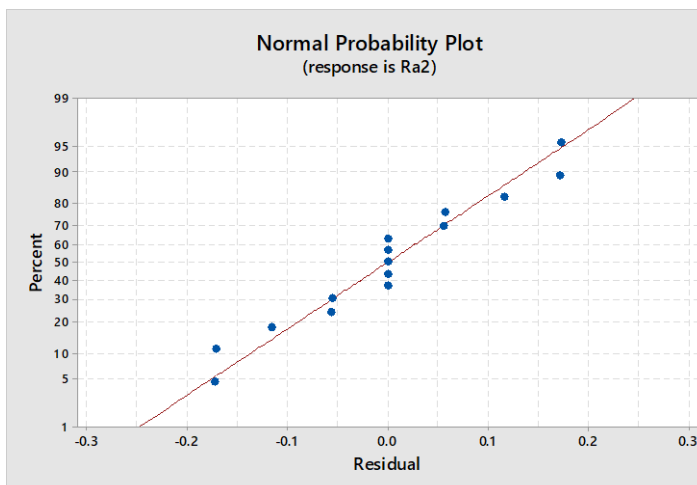


Fig. 4.16

Table. 4.7

ANOVA TABLE for Ra3					
Source	DF	Adj SS	Adj MS	F-Value	P-Value
Model	9	11.1414	1.23793	9.88	0.011
Linear	3	9.0131	3.00437	23.97	0.002
A	1	4.8828	4.88281	38.95	0.002
B	1	3.5258	3.52584	28.13	0.003
C	1	0.6045	0.60445	4.82	0.079
Square	3	1.1386	0.37953	3.03	0.132
A*A	1	0.9571	0.95708	7.64	0.04
B*B	1	0.0483	0.0483	0.39	0.562
C*C	1	0.2342	0.23424	1.87	0.23
2-Way Interaction	3	0.9897	0.32991	2.63	0.162
A*B	1	0.4449	0.44489	3.55	0.118
A*C	1	0.2228	0.22278	1.78	0.24
B*C	1	0.3221	0.32206	2.57	0.17
Error	5	0.6267	0.12535	0.3	0.8
Lack-of-Fit	3	0.6267	0.20891		
Pure Error	2	0	0		
Total	14	11.7681			
Model Summary		S	R-sq	R-sq(adj)	R-sq(pred)
		0.354041	94.67%	85.09%	74.79%

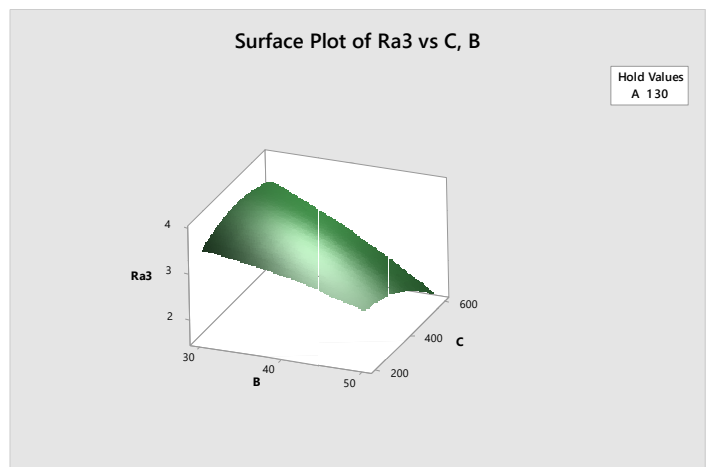


Fig. 4.18 (a)

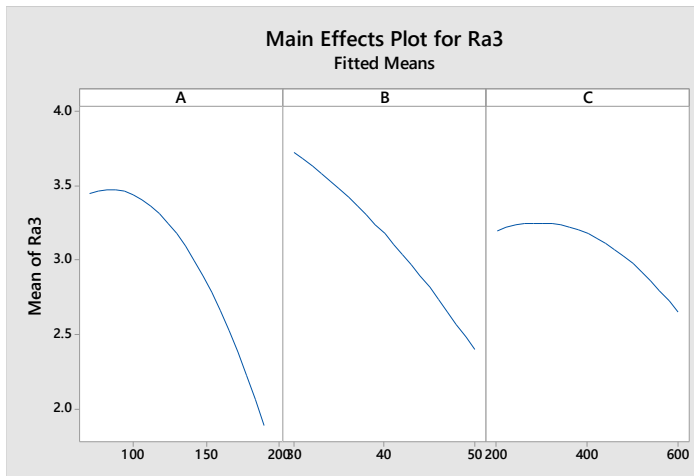


Fig. 4.17

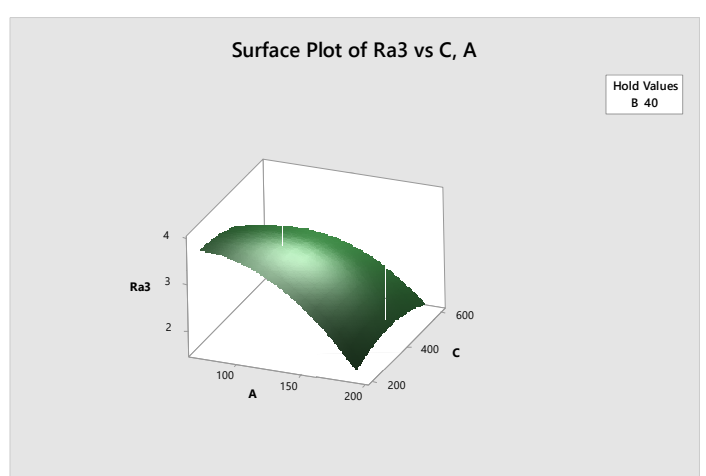


Fig. 4.18(b)

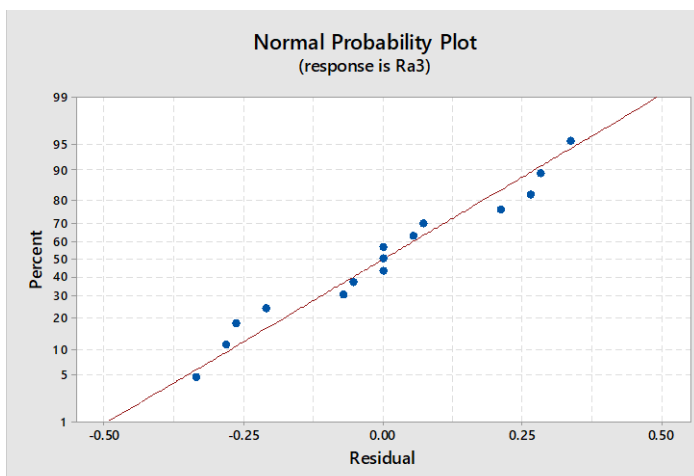


Fig. 4.19

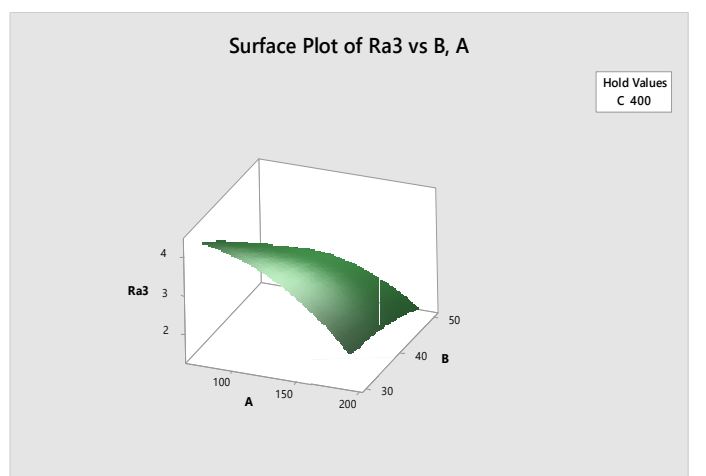


Fig. 4.18(c)

4.3 Roundness Discussion for Spherical Turning (R):-

Roundness is simply the resemblance of the body mathematically with the ideal circle. Measuring the diameter is not same as measuring roundness. Roundness depicts the ratio of the inscribed and the circumscribed circles as per ISO. Roundness measures the mean circle that is bounded between the peak and valley circle as shown in Fig. 4.20; Roundness simply signifies the error that needs to be minimized. In the present study Roundness Tester is used for measuring the roundness of geometry made by spherical turning. Roundness tester is shown in Fig. 3.

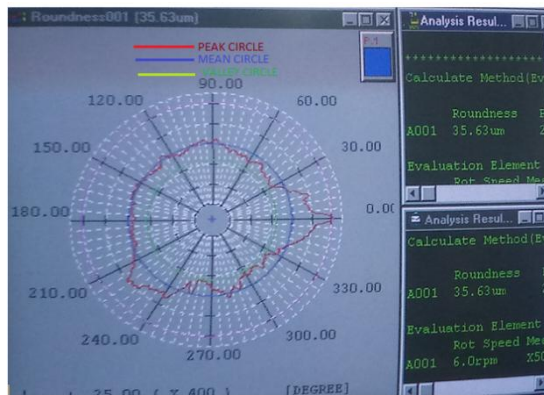


Fig. 4.20 Roundness Circles

Roundness (R) of the 3D shaped probe structure fabricated experimentally for 15 combinations is measured using the Mitutoyo RA 116 Roundness Tester. Table 8 shows the ANOVA table for Roundness and Fig. 4.21, Fig. 4.22 (a, b, c), Fig. 4.23 shows the Individual plots of the factors with R, surface plots between factors and R and Normality plot of R respectively. As shown in the figures, Roundness is most affected by the spindle rotational speed (N) followed by Pulse-off time (Toff) and Gap voltage (GV). R and Toff shows the Inverse relation with roundness whole GV shows direct relation. At low rotational speed more vibration, more spindle errors and machine are encountered that deviate the turning operation from generating the ideal round spherical body and increases the roundness (R). Higher speeds reduces the fluctuations and vibrations by reducing the eccentric effect of the spindle, thus decreases the Roundness (R). Pulse-off time (Toff) also shows the inverse relation with roundness (R) as decrease in Toff leads to increase in surface roughness which deviates the machining envelop causes error in generating the ideal shape and thus increases R value. Gap voltage (GV) shows the direct but least significant behavior with roundness.

Table 4.8

ANOVA TABLE for Roundness					
Source	DF	Adj SS	Adj MS	F-Value	P-Value
Model	9	1552.27	172.47	97.81	0
Linear	3	1383.36	461.12	261.49	0
A	1	75.31	75.31	42.71	0.001
B	1	15.85	15.85	8.99	0.03
C	1	1292.2	1292.2	732.78	0
Square	3	133	44.33	25.14	0.002
A*A	1	0.01	0.01	0	0.959
B*B	1	8.4	8.4	4.76	0.081
C*C	1	127.96	127.96	72.57	0
2-Way Interaction	3	35.9	11.97	6.79	0.033
A*B	1	1.21	1.21	0.69	0.445
A*C	1	34.13	34.13	19.35	0.007
B*C	1	0.56	0.56	0.32	0.597
Error	5	8.82	1.76	0.14	0.63
Lack-of-Fit	3	8.82	2.94		
Pure Error	2	0	0		
Total	14	1561.08			
Model Summary		S	R-sq	R-sq(adj)	R-sq(pred)
		1.32794	99.44%	98.42%	90.96%

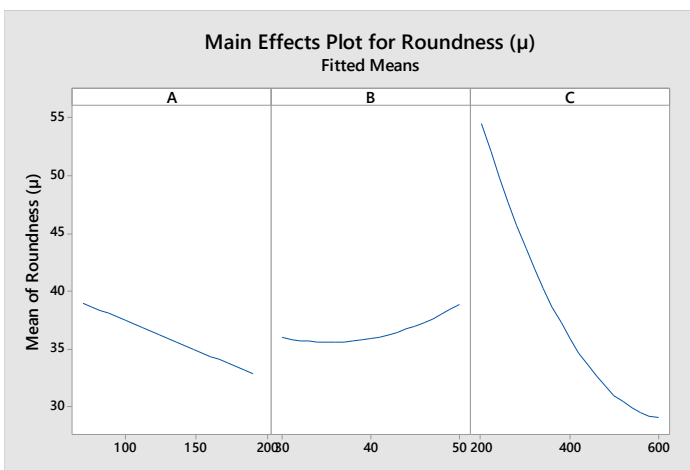


Fig. 4.21

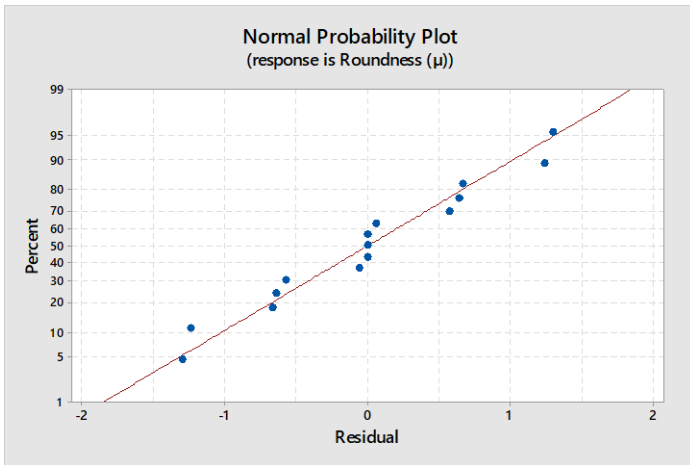


Fig. 4.23

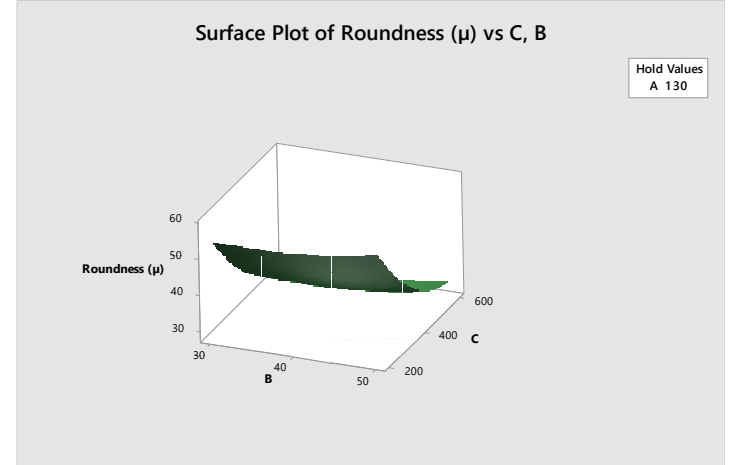


Fig. 4.22 (a)

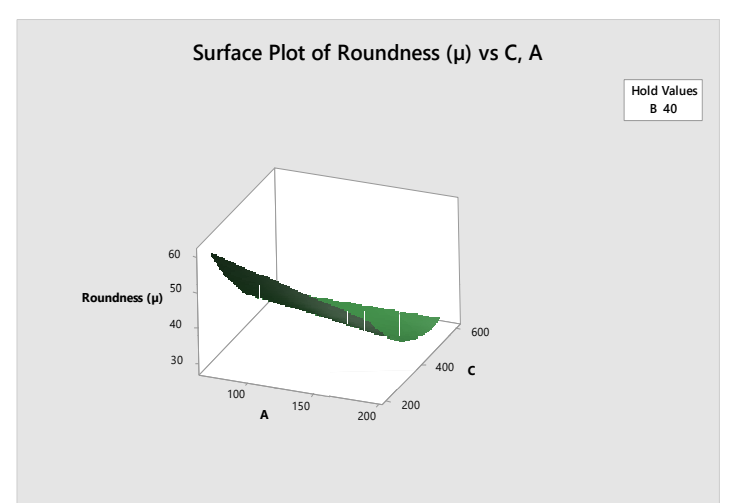


Fig. 4.22 (b)

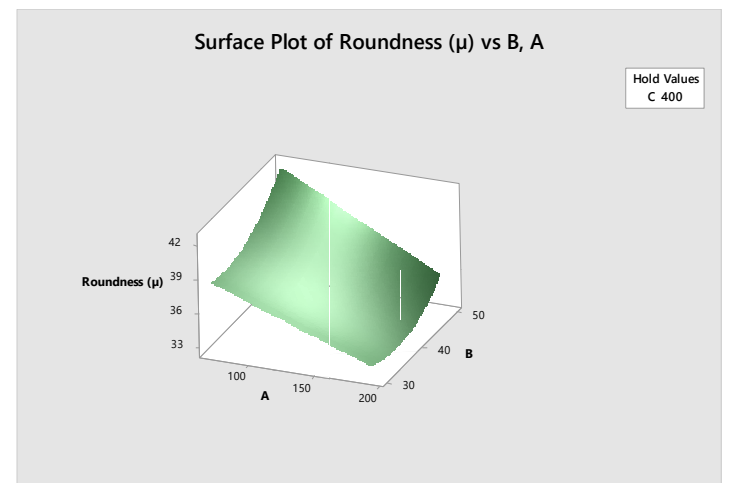


Fig. 4.22 (c)

4.4 Dimensional error Discussion (Δe)

Dimensional error is measured in terms of volume error (mm^3). Volume of the 3D shaped probe structure fabricated is measured using equations α , β and γ derived in section 3.3. Using vernier caliper dimensions of fabricated structure are measured and by putting in formulas obtained in equations α , β and γ , volume V_1 , V_2 and V_3 of each spherical, cylindrical and taper CWEDT geometry is found for each set of experiment. Dimensional error (Δe) is finally calculated by subtracting the volume V_1 , V_2 and V_3 from the Ideal Volume $V_1`$, $V_2`$ and $V_3`$ obtained in section 3.3. **$V_1` = 108.0606 \text{ mm}$, $V_2` = 75.3982$ and $V_3` = 163.3628$ for ideal spherical, cylindrical and taper CWEDT geometry.** Fig.4.24 shows the ideal 3D probe structure and its dimensions.

Δe_1 , Δe_2 , Δe_3 denotes the dimensional error in spherical, cylindrical and taper CWEDT geometries and Δe_T denotes overall dimensional error in fabricated 3D shaped probe geometry and $\% \Delta e$ denotes percentage error in fabricated 3D shaped probe geometry. Table 4.9 below shows dimensional error. It shown that as Gap voltage (GV) INCREASES error increase while on the other hand increase in Spindle speed decreases the dimensional error due to less vibrations and fluctuations high speed rotation (N). Maximum error of 30.85 % and minimum error of 7.9 % is recorded for complete geometric shape.

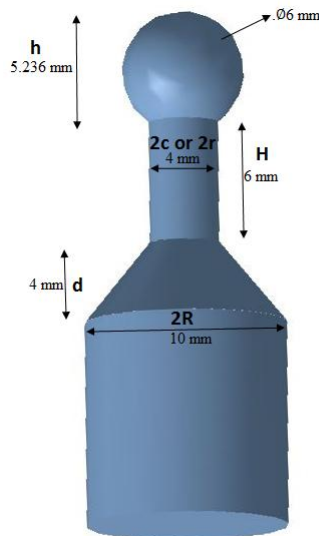


Fig. 4.24

Table 4.9 Dimensional error

Exp. No	Toff	G.V	RPM	$\Delta e1$	$\Delta e2$	$\Delta e3$	ΔeT	% ΔeT
1	190	30	400	22.987	9.8745	5.214	38.0755	10.97
2	70	40	600	11.958	24.245	9.548	45.751	13.19
3	190	40	600	25.2906	22.5182	11.8098	59.6186	17.18
4	190	50	400	24.3498	10.8862	5.5608	40.7968	11.76
5	130	40	400	26.0986	35.7682	19.4678	81.3346	23.45
6	190	40	200	11.6628	16.3445	8.4498	36.4571	10.511
7	130	50	200	28.2976	41.0452	22.7348	92.0776	26.54
8	130	40	400	26.0986	35.7682	19.4678	81.3346	23.45
9	70	30	400	7.1819	13.234	6.987	27.4029	7.9
10	130	50	600	17.5145	38.4532	21.1118	77.0795	22.22
11	130	30	600	17.1639	14.3282	7.3728	38.8649	11.2059
12	130	40	400	26.0986	35.7682	19.4678	81.3346	23.45
13	130	30	200	31.3011	48.2548	27.4788	107.0211	30.85
14	70	50	400	7.9746	14.3262	7.3723	29.6731	8.55
15	70	40	200	18.965	35.235	15.125	69.325	19.98

4.5 Multi-objective Optimization

RSM is used for multi objective optimization. MRR is targeted for maximize, While Surface roughness (Ra) and Roundness are targeted for minimize. Optimization is performed for various categories as listed below:-

1. Multi-Objective response optimization for spherical turning (Fig. 4.25)
2. Multi-Objective response optimization for cylindrical turning (Fig. 4.26)
3. Multi-Objective response optimization for taper turning (Fig. 4.27)
4. Multi-Objective response optimization for 3D shaped probe CWEDT (Fig. 4.28)

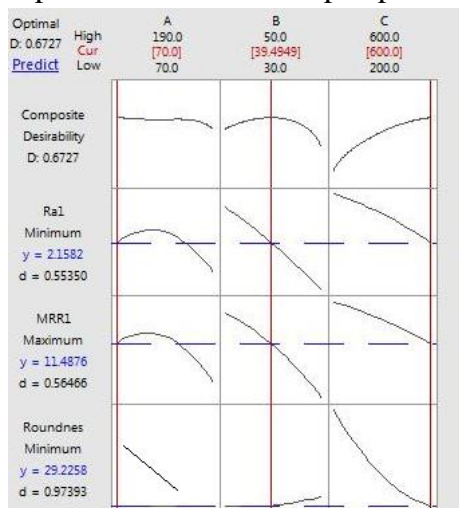
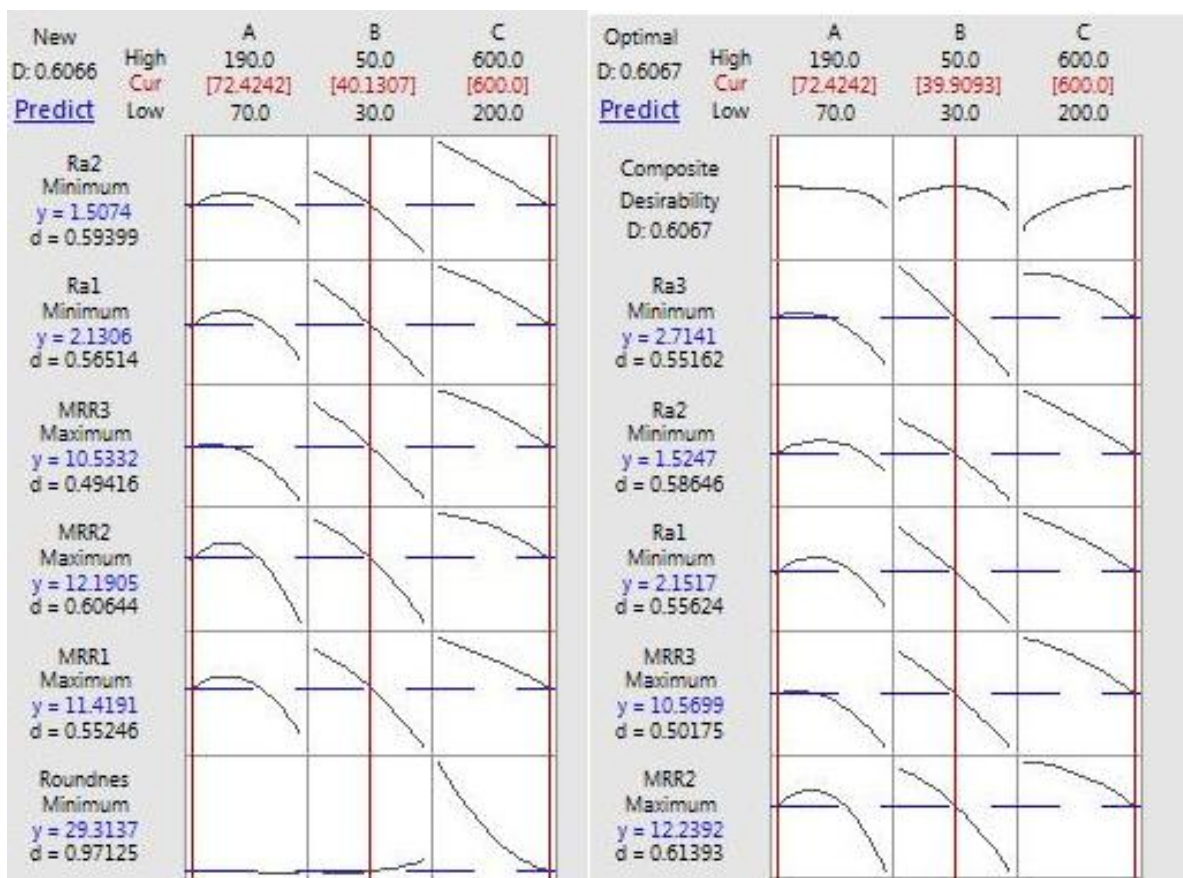
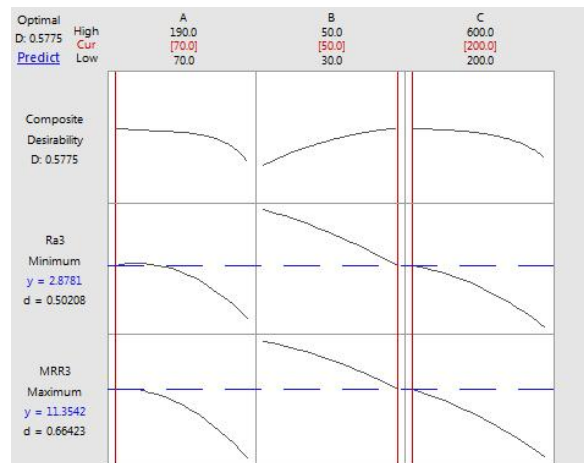
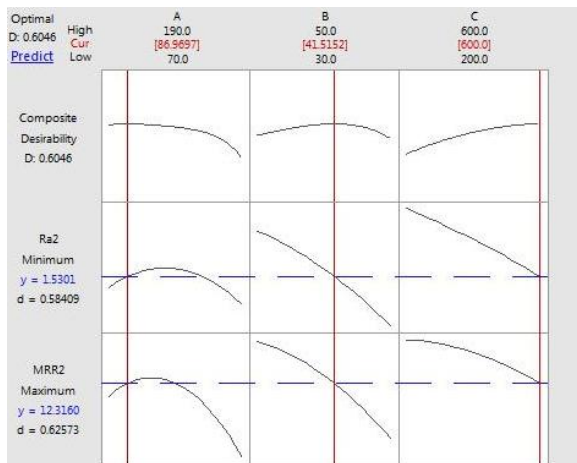


Fig. 4.25 Optimization plot Spherical CWEDT



Optimization plots shown above shows the satisfying values and curves for each of the profile turning. Fig. 4.28 clearly shows the optimum parameters for the full 3D profile fabricated for higher productivity and good surface quality. Values of Pulse OFF (T off), Gap voltage (GV) and Spindle rotation speed (N) for the desired responses are 72.424 μ s, 40.13 V and 600 rpm respectively. Predicted optimum MRR and Ra are 12.2392 mm^3/sec and 1.5247 μm at their best values.

4.6 Confirming Experiments

An Experiment is conducted with the set of parameter obtained in the Multi-objective Optimization performed using response optimizer in section 4.5, below shows the table of parameters obtained in response optimizer.

Table 4.10

Parameter	Predicted Values
Pulse-OFF (Toff)	72.4242 μ s
Gap voltage (GV)	40.1307 V
Spindle speed (N)	600 rpm

Profile generated by the experiment as per parameters shown in Table 4.10 shows the conforming behavior with the predicted model. Response parameters recorded for the experiment is Max MRR= 10.658 mm³/ sec, Min Ra= 1.876 μ m, Roundness for spherical part = 32.134 μ m and dimensional error of 13 %.

From the above conforming experiment data, it is worth noting that conforming experiment shows satisfactory similarity (with error of < 10 %.) with the predicted model given by RSM.

Chapter 5 Conclusions

This chapter contains the concluding statements about the research work conducted on CWEDT. Brief and critical conclusions are made on the basis of chapter 3 Results and Discussion. Process capability of CWEDT is studied by investigating the complex profiles and geometries made as part of 3D probe shaped structure by CWEDT. Fig 5.1 shows the 3D probe shaped structure fabricated by CWEDT.



Fig. 5.1 3D probe shaped structure

Following are the key concluding points:-

- MRR is highly dependent on Gap voltage (GV) followed by Pulse OFF time (Toff), while Spindle rotation speed (N) has the least effect on MRR. MRR rate of Cylindrical Turning is maximum followed by spherical and taper turning. Toff, GV and N all three factors decreases the MRR with their increasing values. Maximum MRR $13.9165 \text{ mm}^3/\text{sec}$ and minimum MRR is $8.14784 \text{ mm}^3/\text{sec}$ is achieved.
- Surface roughness $R_a 1.1\mu\text{m}$ is achieved at high Spindle rotation speed (N) and high Gap voltage (GV). Toff, GV and N all three factors decreases the R_a with their increasing values, thus increases the surface quality. Taper turning shows the least surface finish while cylindrical turning shows high surface finish.
- Roundness (R) is measured for the spherical turned profile. Data shows increasing nature of roundness with low spindle rotation speed (N) and low values of Pulse-off time (Toff). Roundness is highly influenced by the spindle rotation speed (N) followed by pulse-off time (Toff). Gap voltage (GV) shows least significance on roundness. As GV increases roundness increases but very slowly. Min roundness $28.37 \mu\text{m}$ is achieved.
- Mathematical modelling of the 3D probe shaped profile is successfully done and MRR expressions of the complex geometries are derived.

- Dimensional error are measured in terms of volume (mm^3). High values of spindle rotation speed (N) decrease the error. However error increases with GV. Maximum and minimum error calculated were 30.85 % and 7.9 % respectively.
- Multi-Objective response optimization using RSM is done and predicted model with its optimum parameter is generated. For Max. MRR, Min Ra and Min R optimization is done. Predicted set of optimum parameters for spherical turning are $T_{off}= 70 \mu\text{s}$, $GV= 39.49 \text{ V}$ and $N= 600 \text{ rpm}$. For cylindrical turning optimum parameters are $T_{off}= 86.96 \mu\text{s}$, $GV= 41.51 \text{ V}$ and $N= 600 \text{ rpm}$. For Taper turning optimum parameters are $T_{off}= 70 \mu\text{s}$, $GV= 50 \text{ V}$ and $N= 200 \text{ rpm}$.
- Successfully 3D probe shaped structure is fabricated using CWEDT Ra $1.5247 \mu\text{m}$ and minimum dimensional error of 7.9 % with optimum parameters values $72.424 \mu\text{s}$, 40.13 V and 600 rpm of pulse OFF (T off), gap voltage (GV) and spindle rotation speed (N) respectively.
- Confirming Experiments shows satisfactory results with the predicted model with error less than 10 %.

References

1. Ehrfeld, W., Lehr. et al. Micro Electro Discharge Machining as a Technology in Micromachining. SPIE. 2879. (1996) : 332-337
2. Lok, Y. K. and Lee, T. C. Processing of advanced ceramics using the wire-cut EDM process. Journal of Materials Processing Technology. 63(1). (1997) : 839-843
3. Dhake HG and Samuel GL. Machining of axisymmetric forms and helical profiles on cylindrical workpiece using wire cut EDM. Int J Mach Mach Mater. 12(3). (2012): 252–265.
4. Magabe, Sharma et al. Modeling and optimization of Wire-EDM parameters for machining Taguchi and NSGA-II. The International Journal of Advanced Manufacturing Technology. 22. (2019):
5. Kumar, Amit et al. Performance evaluation of Al₂O₃ nano powder mixed dielectric for electric discharge machining of Inconel 825. Materials and Manufacturing Processes 33.9 (2018): 986-995.
6. Muthuramalingam, T., B. Mohan, and A. Jothilingam. Effect of tool electrode resolidification on surface hardness in electrical discharge machining. *Materials and Manufacturing Processes* 29.11-12 (2014): 1374-1380.
7. Qu J, Scattergood RO and Shih AJ. Development of the cylindrical wire electrical discharge machining process, part 1: concept, design, and material removal rate. J Manuf Sci Eng. 124: 702–707. (2002)
8. Qu J, Shih AJ and Scattergood RO. Development of the cylindrical wire electrical discharge machining process, part 2: surface integrity and roundness. J Manuf Sci Eng.124. (2002): 708–714.
9. Haddad MJ, Tajik M, Tehrani AF, et al. An experimental investigation of cylindrical wire electrical discharge turning process using Taguchi approach. Int J Mater Form. 29. (2009): 167–179.
10. Haddad MJ, Alihoseini F, Hadi M, et al. An experimental investigation of cylindrical wire electrical discharge turning process. Int J Adv Manuf Tech; 46. (2010): 1119–1132.
11. Haddad MJ and Tehrani AF. Material removal rate (MRR) study in the cylindrical wire electrical discharge turning (CWEDT) process. J Mater Process Tech. 199 (2008): 369–378.

12. Mohammadi A, Tehrani AF and Abdullah A. Investigation on the effects of ultrasonic vibration on material removal rate and surface roughness in wire electrical discharge turning. *Int J Adv Manuf Tech.* 70 (2014): 1235–1246.
13. Mohammadi A, Tehrani AF, Abdullah A, et al. Investigation of ultrasonic-assisted wire electrical discharge turning based on single discharge analysis. *Proc IMechE, Part B: J Engineering Manufacture.* Epub ahead of print 12 February 2014.
14. Aminollah Mohammadi, Alireza Fadaei Tehrani & Amir Abdullah. Modelling and optimisation of the process parameters in ultrasonic-assisted wire electrical discharge turning. *Advances in Materials and Processing Technologies.* 2016. 10.1080/2374068X.2015.1127533.
15. Janardhan V and Samuel GL. Pulse train data analysis to investigate the effect of machining parameters on the performance of wire electro discharge turning (WEDT) process. *Int J Mach Tool Manu.* 50. (2010) :775–788.
16. Abimannan Giridharan & G. L. Samuel. Investigation into erosion rate of AISI 4340 steel during wire electrical discharge turning process. *Machining Science and Technology.* 2017. 10.1080/10910344.2017.1365890.
17. Sun, Gong et al. Experimental study on surface characteristics and improvement of microelectrode machined by low speed wire electrical discharge turning. *archives of civil and mechanical engineering.* 17 .(2017) : 964–977.
18. Yao Sun, Yadong Gong. Experimental study on the microelectrodes fabrication using low speed wire electrical discharge turning (LS-WEDT) combined with multiple cutting strategy. *Journal of Materials Processing Tech.* 250. (2017) :121–131.
19. Vikas Gohil, Y. M. Puri. Optimization of Electrical Discharge Turning Process using Taguchi-Grey Relational Approach. *Procedia CIRP.* 68. (2018) : 70 – 75.
20. Chen, Wang. et al. Micro reciprocated wire-EDM of micro-rotating structure combined multi-cutting strategy. *The International Journal of Advanced Manufacturing Technology.* 2018. 10.1007/s00170-018-2145-0
21. D. Balamurali, K. Manigandan, V. Sridhar. Analysis of the Effect of Machining Parameters on Wire Electrical Discharge Turning of Stainless Steel. *Journal of Advanced Engineering Research.* 2. (2015) : 34-41.
22. Srivastava AK, Nag. et al. Surface integrity in wire-EDM tangential turning of in situ hybrid metal matrix composite A359/B4C/Al₂O₃. *J.Science engineering and Composite Material.* 2018.

23. Rajurkar, K. P. and Pandit, S. M., 1988, "Recent Progress in Electrical Discharge Machine Technology and Research," Proceedings of Manufacturing International.88, Atlanta, GA, USA. 1. (1988): 219-226.
24. Poco, 2000, EDM Technoloy Manual, Poco Graphite Inc.
25. T.A. Spedding, Z.Q. Wang, Study on modelling of wire EDM process, *J. Mater. Process. Technol.* 69 (1997) : 18-28.
26. Mahapatra, S. S. and Patnaik, A. Optimization of wire electrical discharge machining process parameters using Taguchi method, *International Journal of Advanced Manufacturing Technology* 34(9-10). (2007) : 911-925.
27. Patel JD, Maniya KD (2018) A review on: wire cut electrical discharge machining process for metal matrix composite. *Procedia Manuf* 20:253–258 (process parameters)